Status of Ensemble Forecasting at ECMWF: 32-day seamless probabilistic prediction

Roberto Buizza[1]

Acknowledgements to Frederic Vitart[1], Martin Leutbecher[1], Jean Bidlot[1], Ersagun Kuscu[1] and Young-Youn Park[1,2]

(1): European Centre for Medium-Range Weather Forecasts
(2) Korea Meteorological Administration

ECMWF supporting and co-operating states

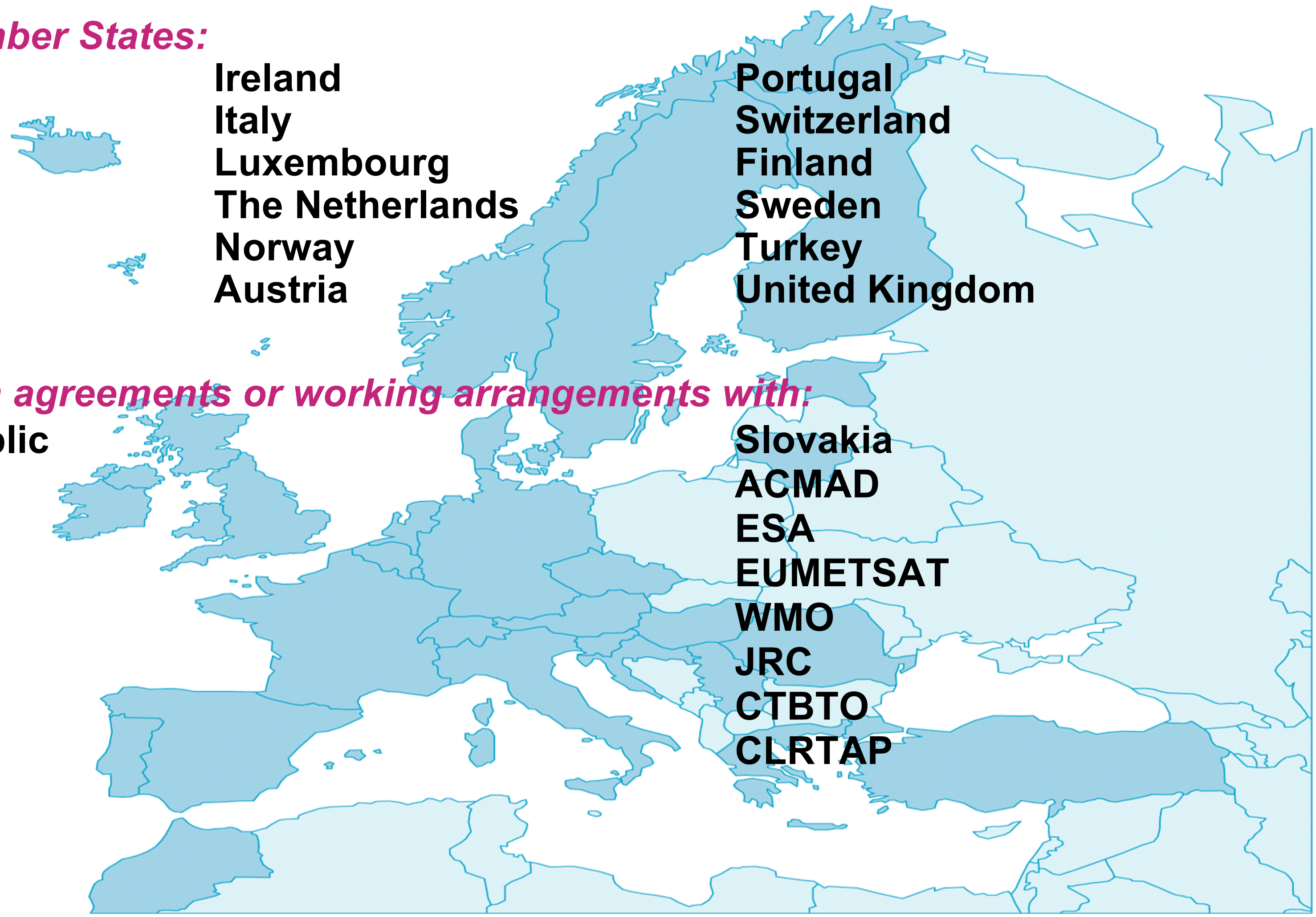

ECMWF Member States:

Belgium
Denmark
Germany
Spain
France
Greece
Ireland
Italy
Luxembourg
The Netherlands
Norway
Austria
Portugal
Switzerland
Finland
Sweden
Turkey
United Kingdom

Co-operation agreements or working arrangements with:

Czech Republic
Croatia
Estonia
Hungary
Iceland
Lithuania
Montenegro
Morocco
Romania
Serbia
Slovenia
Slovakia
ACMAD
ESA
EUMETSAT
WMO
JRC
CTBTO
CLRTAP

ECMWF objectives

- Operational forecasting (including waves) from days to seasons ahead
- Research and development activities in forecast modelling
- Data archiving and related services
- Advanced training in numerical weather prediction
- Provision of supercomputer resources
- Assistance to WMO programmes
- Management of Regional Meteorological Data Communications Network (RMDCN)

ECMWF budget (2006)

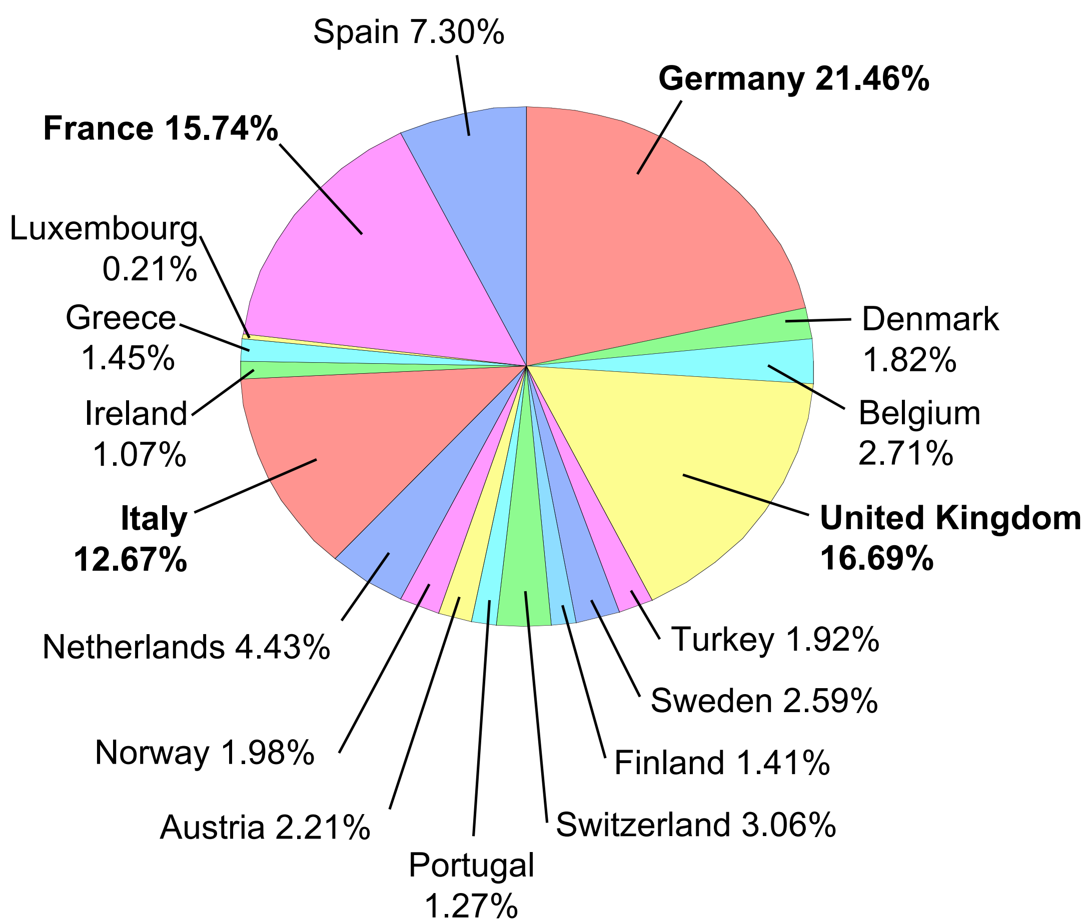

GNI Scale 2006–2008

Main Revenue 2006

Member States' contributions	£27,460,600
Co-operating States' contributions	£425,100
Other Revenue	£1,454,600
Total	**£29,340,300**

Main Expenditure 2006

Staff	£12,961,900
Leaving Allowances & Pensions	£1,807,500
Computer Expenditure	£11,785,900
Buildings	£1,858,000
Supplies	£927,000
Total	**£29,340,300**

Outline

1. The rationale for a probabilistic approach to weather prediction
2. The ECMWF 32-day VAREPS/monthly ensemble system
3. Average performance of the ECMWF ensemble
4. Seamless probabilistic prediction:
   - Weekly-average predictions over Europe (March-April ’08)
   - Prediction of intense rainfall in Portugal and Spain (18-20 April ’08)
   - Prediction of cyclone Nargis (2-3 May 2008)
5. Future changes and conclusions

1. The ECMWF Numerical Weather Prediction Model

The behavior of the atmosphere is governed by a set of physical laws which express how the air moves, the process of heating and cooling, the role of moisture, and so on.

Interactions between the atmosphere and the underlying land and ocean are important in determining the weather.

ECMWF MODEL / ASSIMILATION SYSTEM

ATMOSPHERE	STRATOSPHERE	DYNAMICS–RADIATION–SIMPLIFIED CHEMISTRY		
	TROPOSPHERE	DYNAMICS–RADIATION–CLOUDS–ENERGY & WATER CYCLE		
OCEAN / LAND		OCEAN	LAND HYDROSPHERE	LAND BIOSPHERE
		OCEAN SURFACE WAVES OCEAN CIRCULATION SIMPLIFIED SEA ICE	SNOW ON LAND SOIL MOISTURE FREEZING	LAND SURFACE PROCESSES SOIL MOISTURE PROCESSES SIMPLIFIED VEGETATION

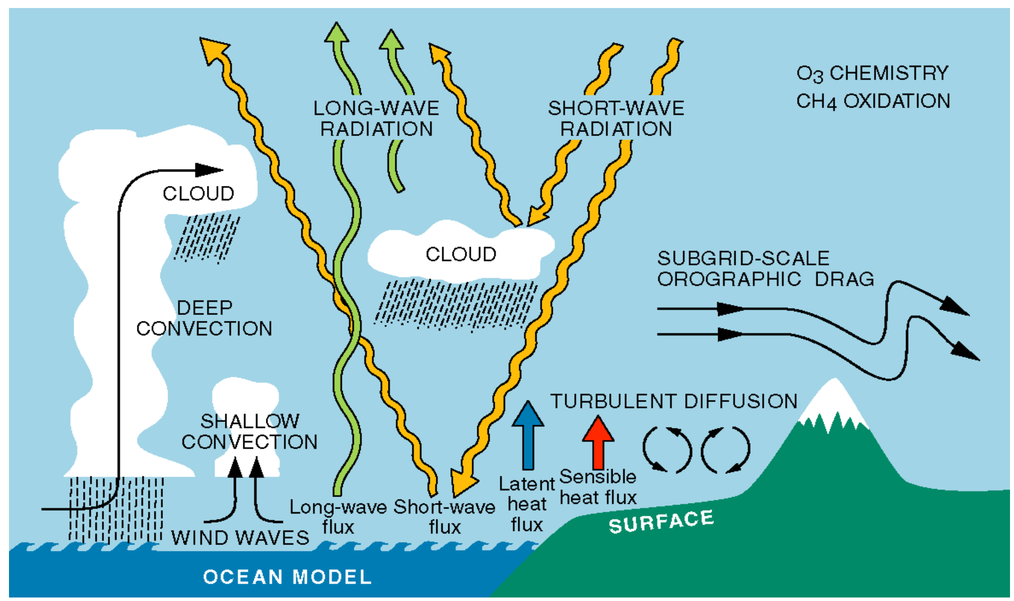

1. Starting a NWP: the initial conditions

To make accurate forecasts it is important to know the current weather:

- observations covering the whole globe are continuously downloaded and fed into the system;
- about 600,000 observations are processed every 12 hours;
- complex assimilation procedures are used to optimally define the initial state of the system.

Unfortunately, very few observations are taken in some regions of the world (e.g. polar caps, oceans).

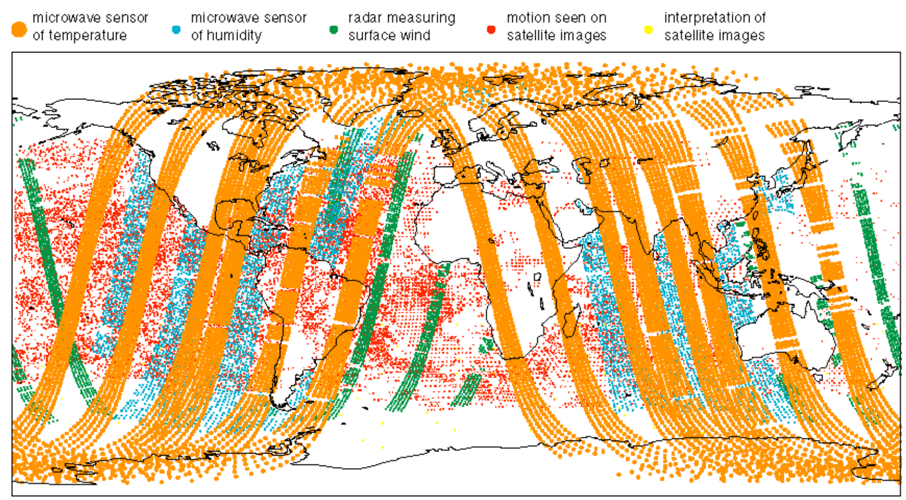

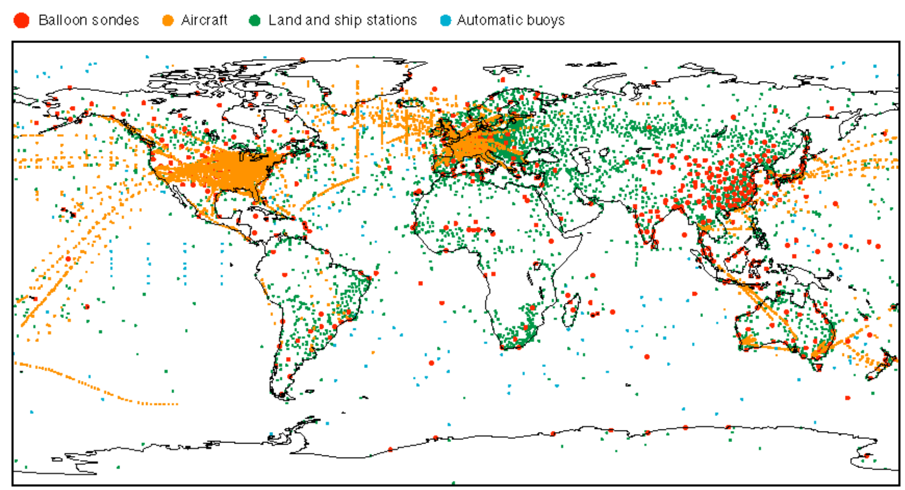

1. Sources of fc errors: initial and model uncertainties

Weather forecasts lose skill because of the growth of errors in the initial conditions (initial uncertainties) and because numerical models describe the laws of physics only approximately (model uncertainties). As a further complication, predictability (i.e. error growth) is flow dependent. The Lorenz 3D chaos model illustrates this.

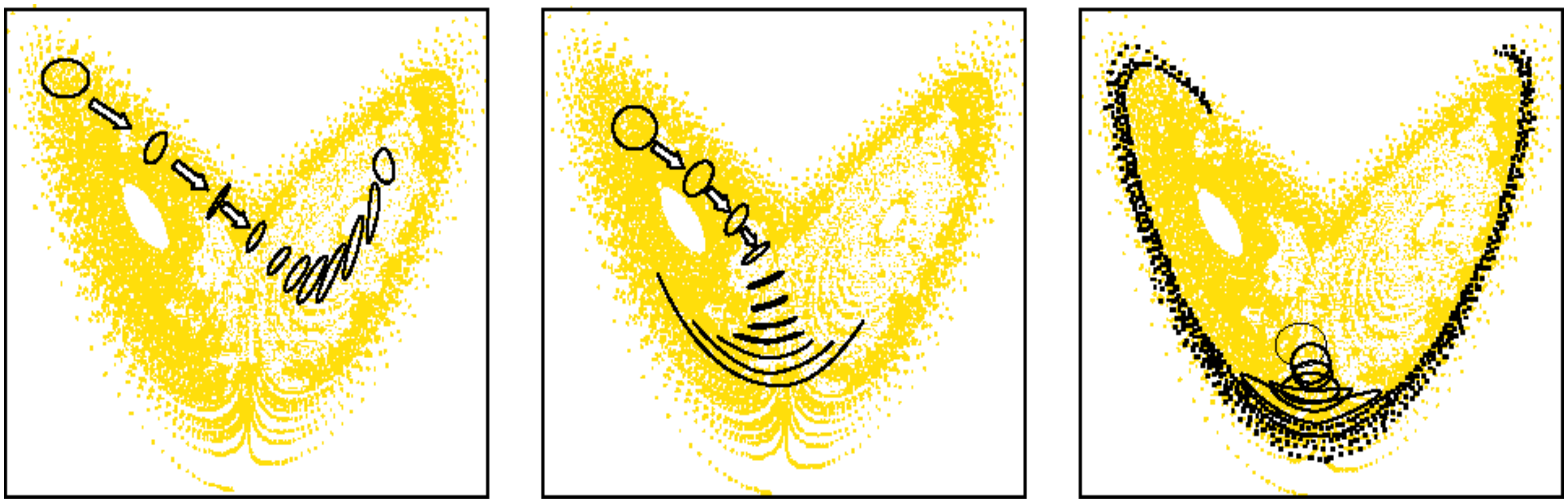

1. The atmosphere's chaotic behavior: an example

A dynamical system shows a chaotic behavior if most orbits exhibit sensitivity to initial conditions, i.e. if most orbits that pass close to each other at some point do not remain close to it as time progresses.

This figure shows the verifying analysis (top-left) and 15 132-hour forecasts of mean-sea-level pressure started from slightly different initial conditions (i.e. from initially very close points).

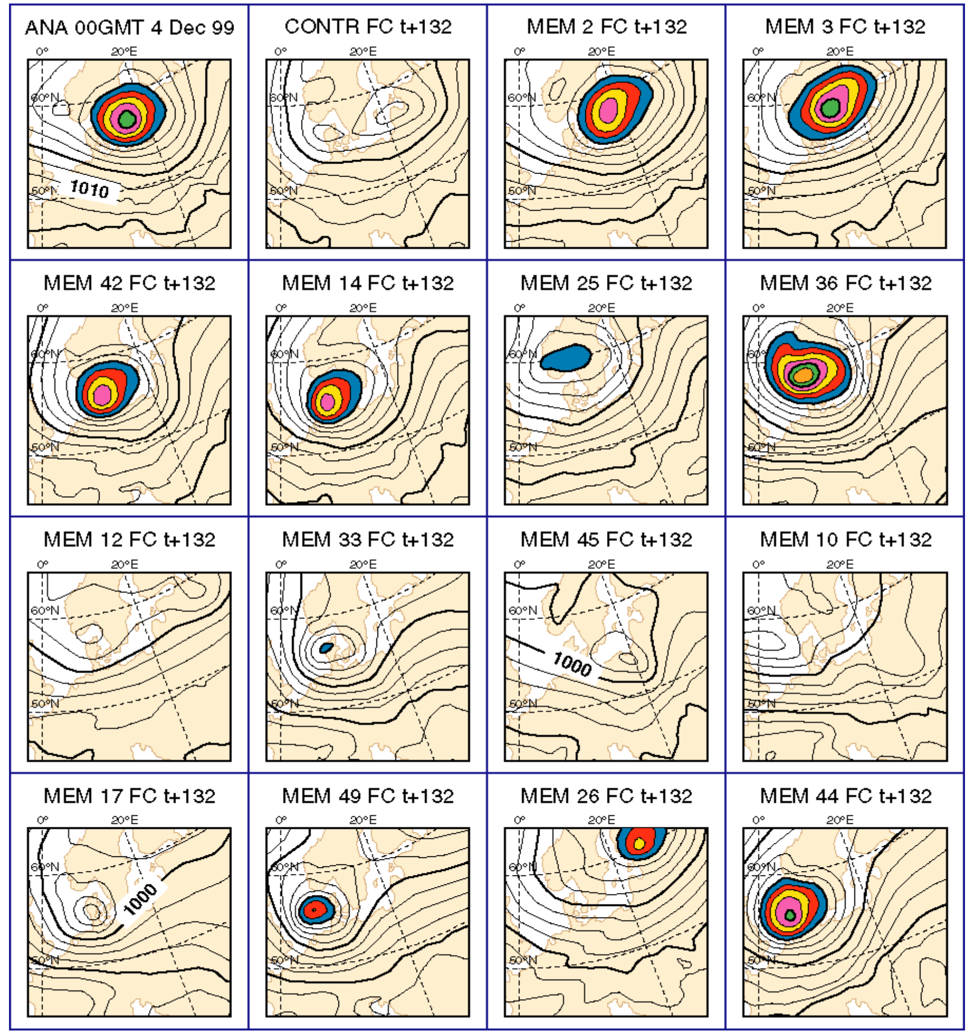

1. Predictability is flow dependent: spaghetti plots

The degree of mixing of Z500 isolines is an index of low/high perturbation growth.

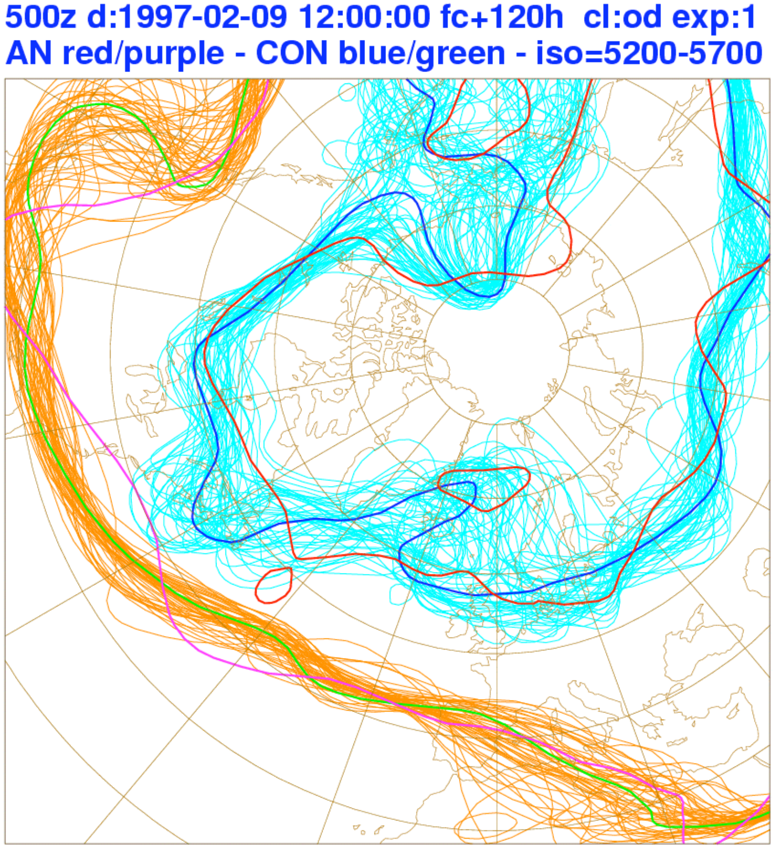

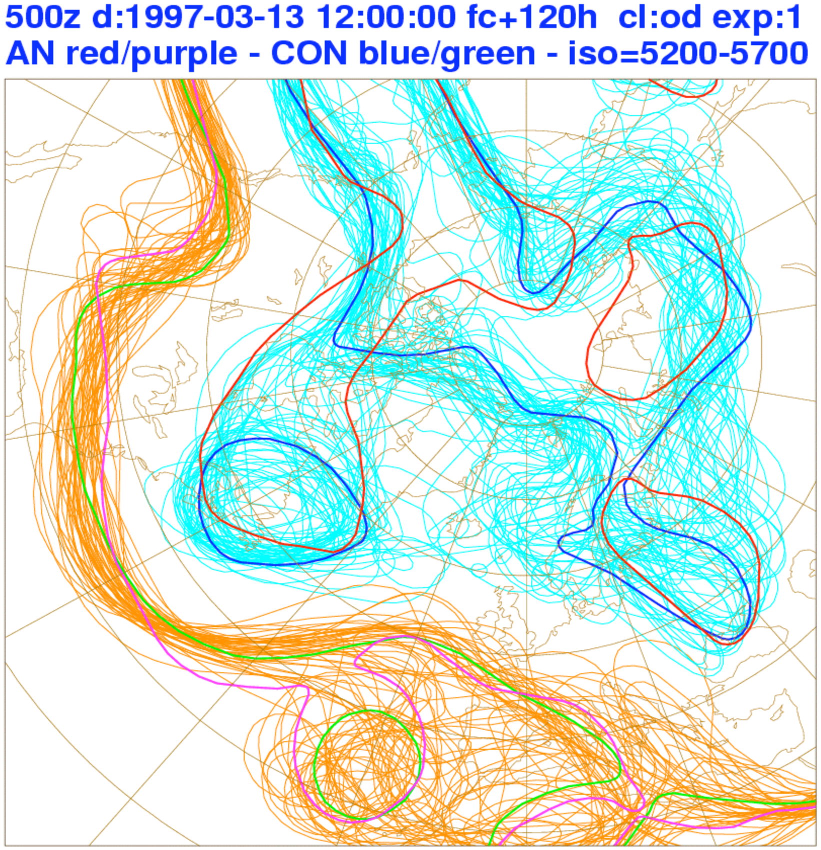

1. Schematic of ensemble prediction

Two are the main sources of error growth: initial and model uncertainties.

Predictability is flow dependent.

A complete description of weather prediction can be stated in terms of an appropriate probability density function (PDF). Ensemble prediction based on a finite number of deterministic integration appears to be the only feasible method to predict the PDF beyond the range of linear growth.

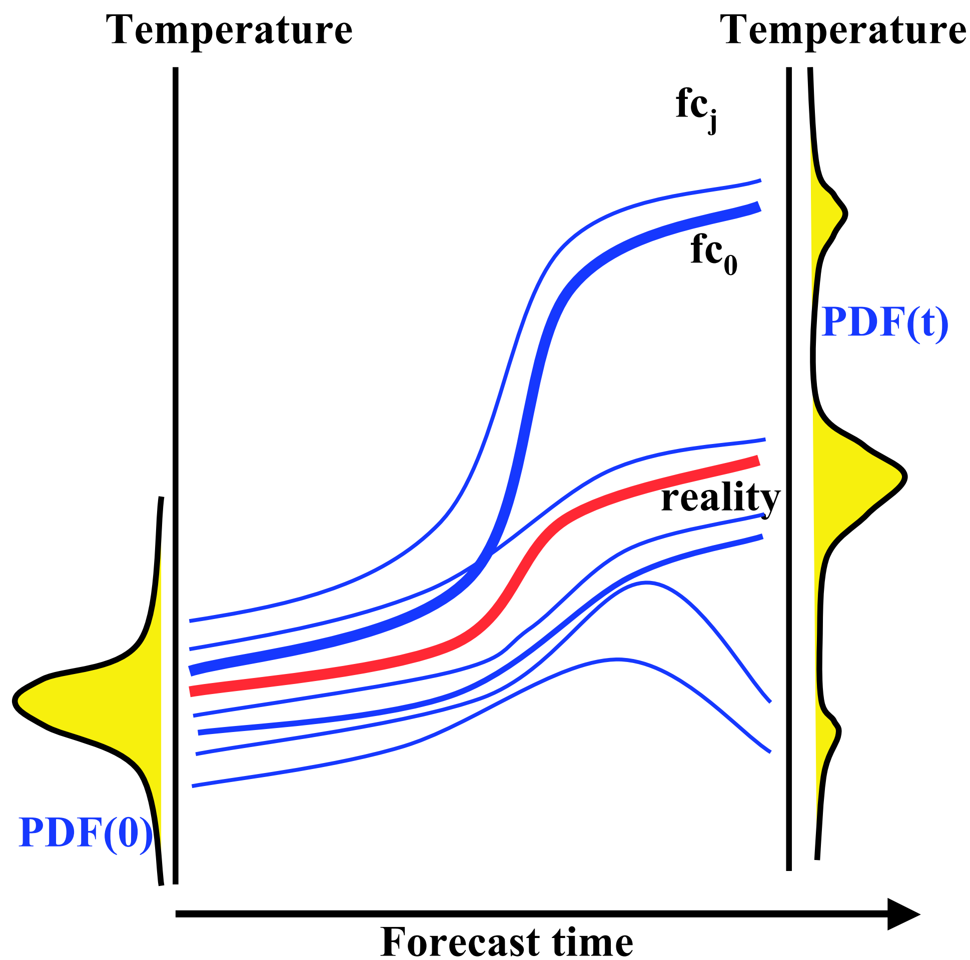

1. How should initial uncertainties be defined?

Perturbations pointing along different axes in the phase-space of the system are characterized by different amplification rates. As a consequence, the initial PDF is stretched principally along directions of maximum growth.

The component of an initial perturbation pointing along a direction of maximum growth amplifies more than a component along another direction (*Buizza & Palmer* 1995).

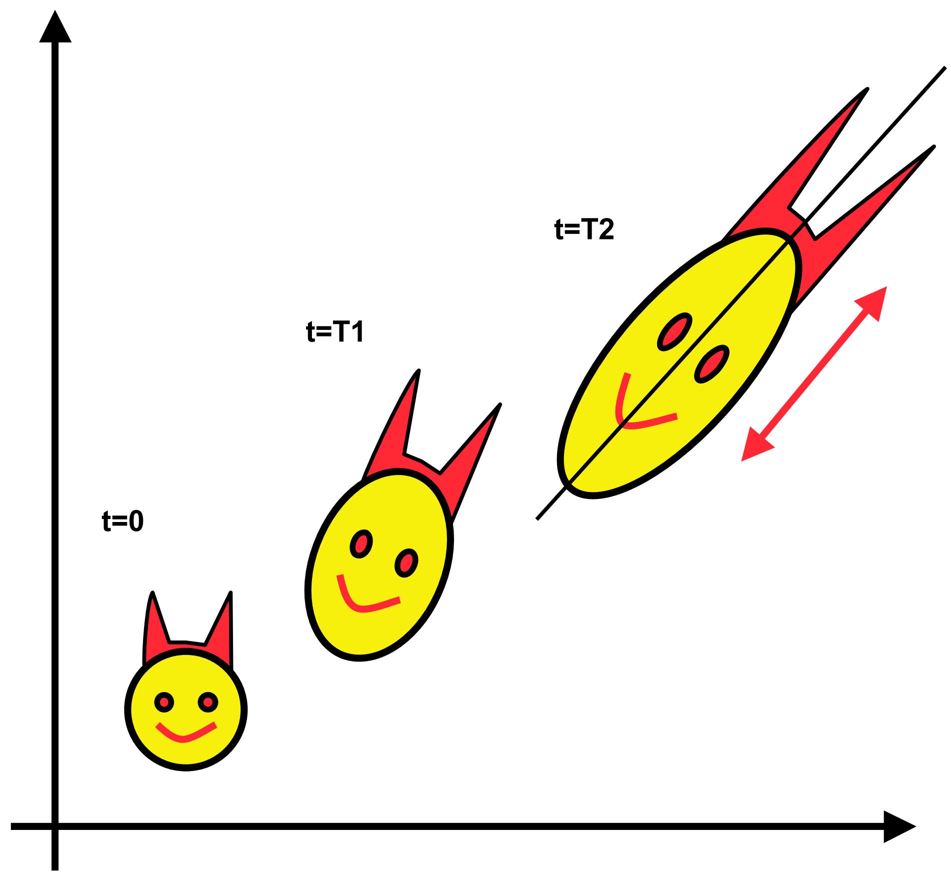

1. SV definition: total-energy metric (and norm)

Given two state-vectors *x* and *y* expressed in terms of vorticity ζ, divergence *D*, temperature *T*, specific humidity *q* and surface pressure π, the total energy metric (and the associated norms) is defined (<..,..> is the Euclidean inner product) as:

$$< x; E_{TE} y >= \frac{1}{2}\iint (\nabla\Delta^{-1}\zeta_x \cdot \nabla\Delta^{-1}\zeta_y + \nabla\Delta^{-1}D_x \cdot \nabla\Delta^{-1}D_y + \frac{C_p}{T_r} T_x T_y) d\Sigma \frac{\partial p}{\partial \eta} d\eta$$

$$+ \int (R_d \frac{T_r}{p_r} \ln\pi_x \ln\pi_y) d\Sigma$$

1. SV definition: the adjoint operator

Given any two vectors *x* and *y*, the adjoint operator L^* of the linear operator *L* with respect to the Euclidean norm <..,..> is the operator that satisfies the following property:

$$< L^* x; y >=< x; Ly >$$

Using the adjojnt operator L^* the time-t E-norm of z′ can be written as:

$$\left\| z'(t) \right\|^2 =< Lz'_0; ELz'_0 >=< z'_0; L^* ELz'_0 >$$

1. SV definition: the linearized model equations

Consider an N-dimensional system:

$$\frac{\partial y}{\partial t} = A(y)$$

Denote by z' a small perturbation around a time-evolving trajectory z:

$$\frac{\partial z'}{\partial t} = A_l(z)z' \qquad A_l(z) = \left.\frac{\partial A(z)}{\partial z}\right|_z$$

$$\frac{\partial z}{\partial t} = A(z)$$

The time evolution of the small perturbation z' is described to a good degree of approximation by the linearized system $A_l(z)$ defined by the trajectory. Note that the trajectory is not constant in time.

1. SV definition: the eigenvalue problem

The solution of the linearized system can be written in terms of the linear propagator *L(t,0)*:

$$z'(t) = L(t,0)z'_0$$

The linear propagator is defined by the system equations and depends on the trajectory characteristics.

The E-norm of the perturbation at time *t* is given by:

$$\|z'(t)\|^2 = < z'(t); Ez'(t) > = < L(t,0)z'_0; EL(t,0)z'_0 >$$

1. SV definition: the eigenvalue problem

The computation of the directions of maximum growth can be stated as 'finding the directions in the phase-space of the system characterized by the maximum ratio between the time-t and the initial norms':

$$\max_{x_0 \in \Sigma} \frac{\|x(t)\|_E^2}{\|x_0\|_{E_0}^2} = \max_{x_0 \in \Sigma} \frac{< x_0; L^* E L x_0 >}{< x_0; E_0 x_0 >}$$

The problem reduces to solving the following eigenvalue problem:

$$E_0^{-1/2} L^* E L E_0^{-1/2} \nu = \sigma^2 \nu$$

1. SVs' geographical distributions and Eady index

The geographical distribution of the singular vectors reflect the characteristics of the underlying basic-state flow. A measure of the baroclinic instability of the basic-state flow is given by the Eady index:

$$\sigma_E = 0.31 \frac{f}{N} \frac{du}{dz}$$

which is the growth rate of the most unstable Eady mode (*Hoskins & Valdes* 1990). In this equation, the static stability N and the vertical wind shear can be estimated using the 300- and 1000-hPa potential temperature and wind. Results indicate that locations with maximum singular vector concentration coincide with regions with maximum Eady index.

1. Example: singular vectors for 18-20 Jan 1997

This figure shows the amplification rate (i.e. the singular value) of the leading 30 unstable singular vectors growing between 18 and 20 January 1997. The SVs were computed at the resolution T42L31 and were used to generate the EPS initial conditions.

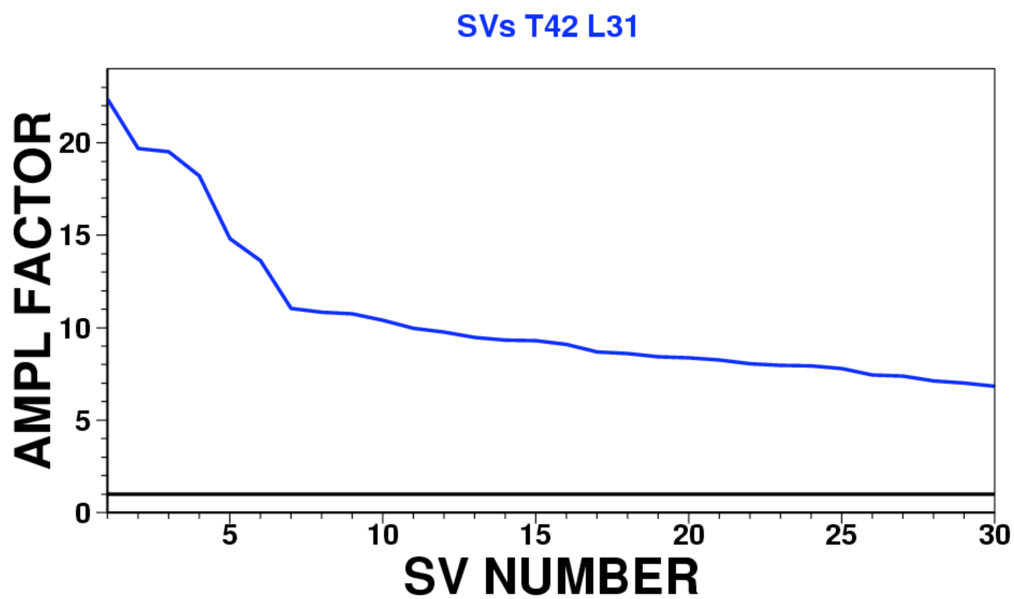

1. Example: singular vector 1 for 18-20 Jan 1997

This figure shows the most unstable singular vector growing between 18 and 20 Jan 1997.

Left (right) panels show the SV at initial and final (i.e. +48h) time.

The top panels show the SV T at model level 18 (~500hPa, shading) and the Z500 analysis; the bottom panels the SV T at model level 23 (~700hPa, shading).

The contour interval is 8dam for Z, and 0.01 (0.05) deg for T at initial (final) time (the SV is normalized to have unit total energy norm at initial time).

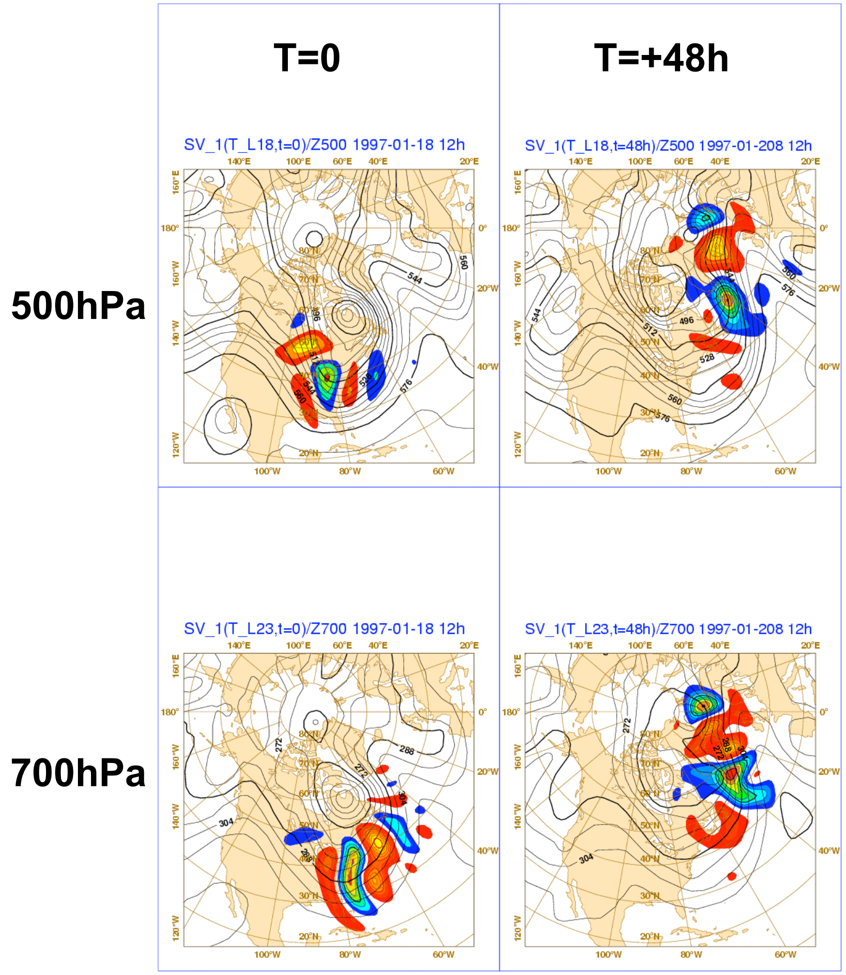

1. Example: vertical X section of SV 1 for 18-20 Jan 1997

This figure shows, for SV 1, the vertical cross section of the T component at initial time (top, for 36N) and of the vorticity component at final time (bottom, for 44N).

The two cross sections have been taken along the parallel where the SV had maximum amplitude. Note the strong initial tilt, suggesting baroclinic instability, and the final time more barotropic-type structure.

Note that T is shown at initial time and vor at final time because the initial time SV has a strong potential energy part.

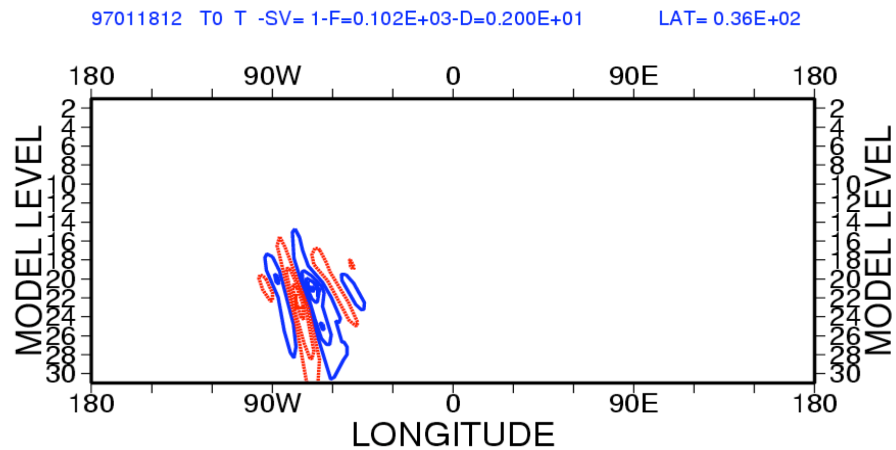

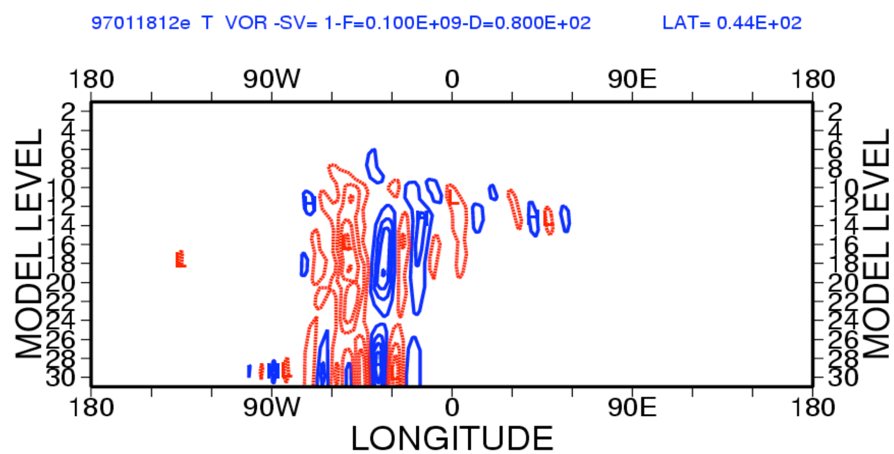

1. Example: energy distr. of SV 1 for 18-20 Jan 1997

The top figure shows, for SV 1, the vertical distribution at initial time of the kinetic (red dotted, x100) and total (red solid, x100) energy, and the corresponding final time distributions (blue).

The bottom figure shows the total energy spectrum at initial (red solid, x100) and at final time (blue solid).

Note the upward and upscale energy transfer/growth, and the transformation from initial potential to mainly final kinetic energy.

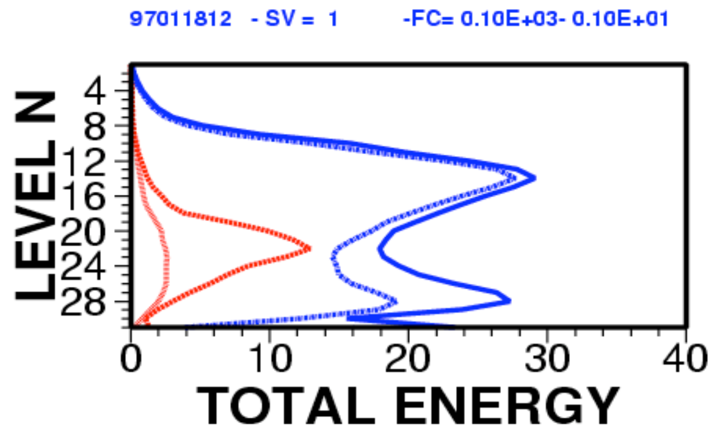

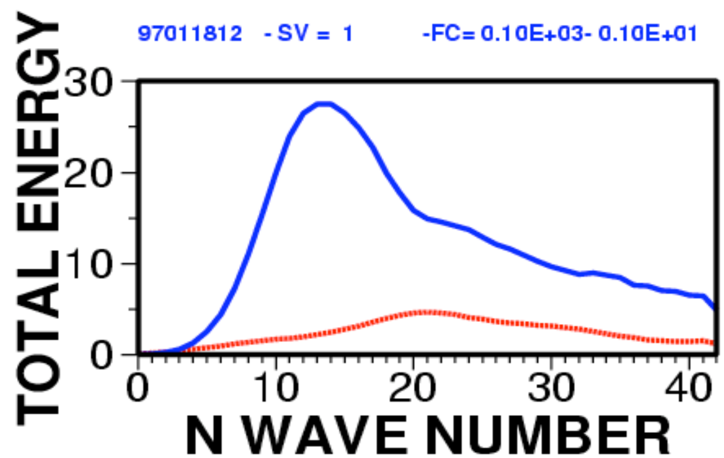

1. Example: average energy distr. for 18-20 Jan 1997

The top figure shows the SV1:25 average vertical distribution at initial time of the kinetic (red dotted, x100) and total (red solid, x100) energy, and the corresponding final time distributions (blue).

The bottom figure shows the SV1:25 average total energy spectrum at initial (red solid, x100) and at final time (blue solid).

Note the SV typical upward and upscale energy transfer/growth, and the transformation from initial potential to mainly final kinetic energy.

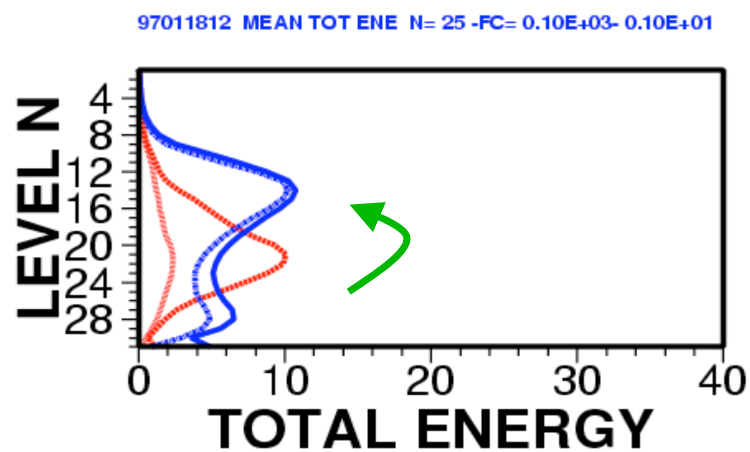

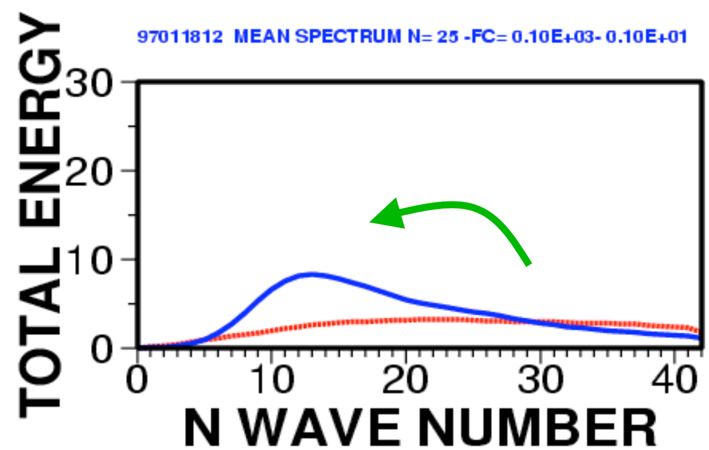

1. Example: SVs' and Eady index for 18-20 Jan 1997

The top panel shows the t+24h average root-mean-square (rms) amplitude (in terms of Z500) of the first 25 singular vectors growing between 18 and 20 January 1997.

The bottom panel shows the 18-20 January 1997 average Eady index.

The contour isolines are 0.5dam for the SV's rms amplitude and 0.5d^{-1} for the Eady index. Results indicate a good correspondence between areas of SV concentration and of maximum value of the Eady index.

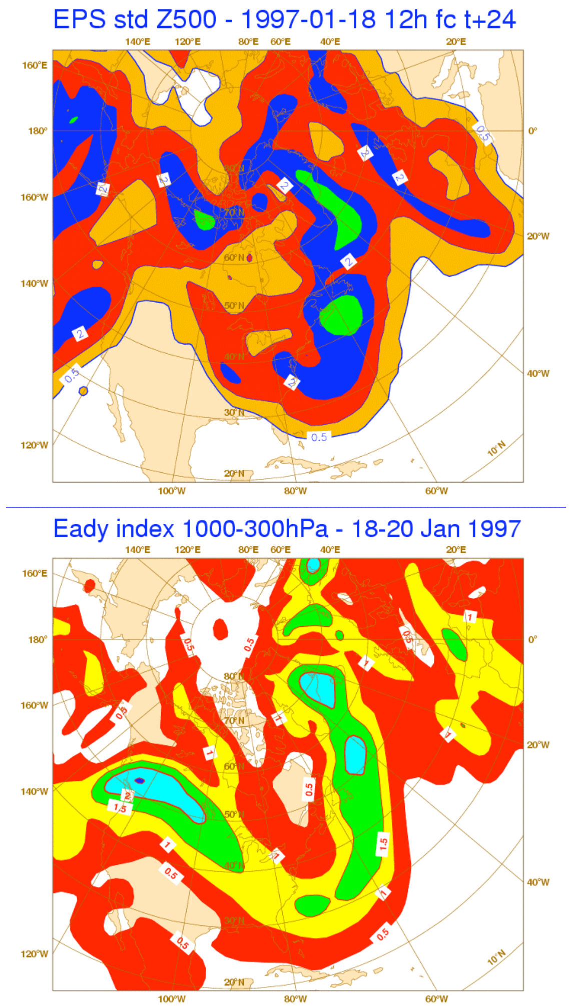

1. Example: NH SVs & Eady index - JFM 1997 and 1998

The top panels show the average t+24h root-mean-square amplitude (in terms of Z500, ci=0.3dam) of the first 25 singular vectors during JFM 1997 (left) and 1998 (right) over the NH.

The bottom panels show the average Eady index computed between 1000 and 300 hPa (ci=0.2d^{-1}).

Results indicate a good agreement between areas of large Eady index and high SV concentration.

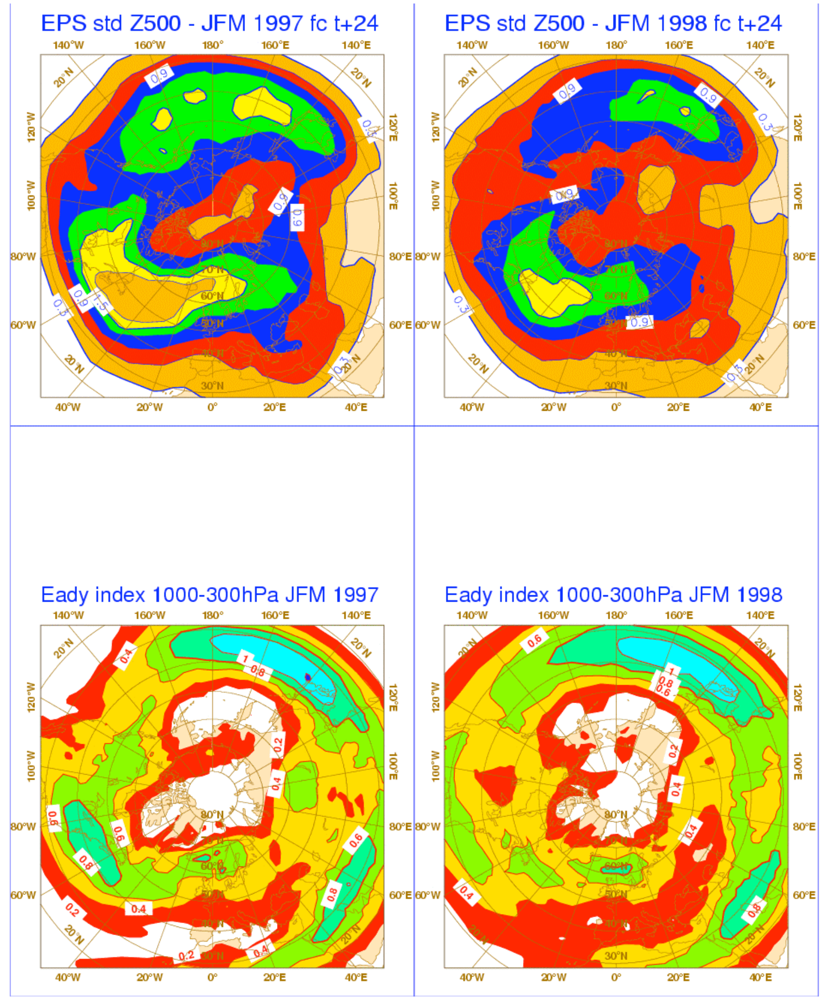

Outline

1. The rationale for a probabilistic approach to weather prediction
2. The ECMWF 32-day VAREPS/monthly ensemble system
3. Average performance of the ECMWF ensemble
4. Seamless probabilistic prediction:
   - Weekly-average predictions over Europe (March-April ’08)
   - Prediction of intense rainfall in Portugal and Spain (18-20 April ’08)
   - Prediction of cyclone Nargis (2-3 May 2008)
5. Future changes and conclusions

2. The operational ECMWF probabilistic system

The medium-range probabilistic system consists of 51 forecasts run with variable resolution:

- T_L399L62 (~50km, 62 levels) from day 0 to 10
- T_L255L62 (~80km, 62 levels) from day 10 to 15/32

The EPS is run twice a-day, at 00 and 12 UTC.

Initial uncertainties are simulated by perturbing the unperturbed analyses with a combination of T42L62 singular vectors, computed to optimize total energy growth over a 48h time interval.

Model uncertainties are simulated by adding stochastic perturbations to the tendencies due to parameterized physical processes.

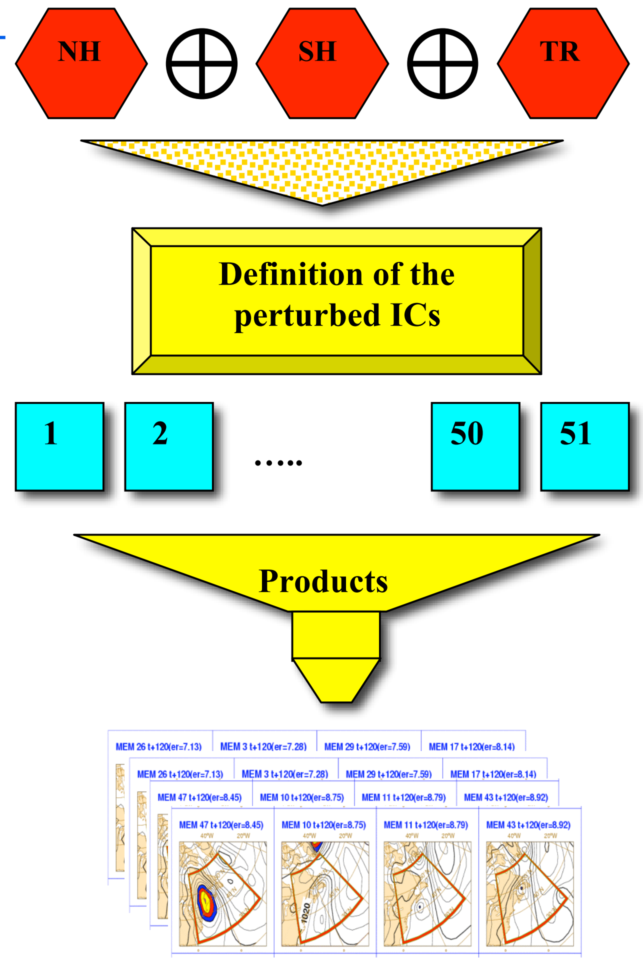

1. The 2008 seamless VAREPS/monthly ensemble system

On the 11th of Mar '08 the 15-day VAREPS was merged with the monthly forecast system: since then the daily 00 UTC forecasts use a coupled ocean model from day 10 to day 15 (day 32 once a week).

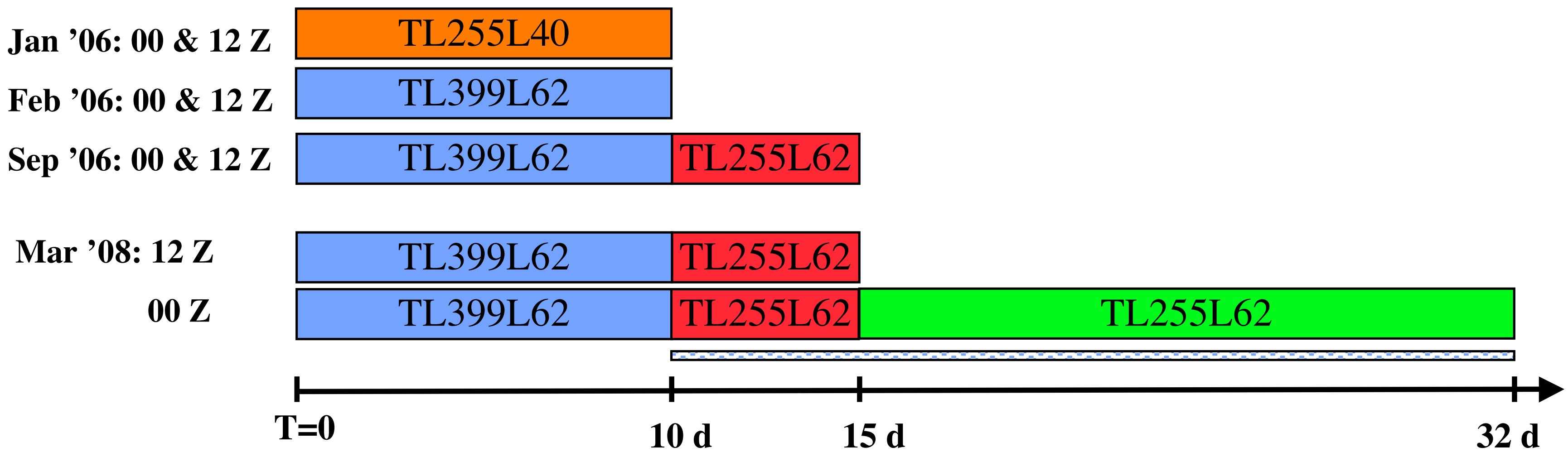

2. Since its introduction the ensemble changed 16 times

Since its implementation the ECMWF system changed several times: ~50 model cycles (these included changes in the model and DA system) were implemented, and the EPS configuration was modified 16 times, e.g.:

- Dec 1992: the ensemble started with 33 members run for 10 days, three times a week only (starting at 12UTC on Fri-Sat-Sun)
- May 1994: from 1 May 1994 the ensemble has been run every day
- Sep 2006: the ensemble forecast range was extended to 15 day (VAREPS)
- March 2008: the 15-day VAREPS and the coupled monthly have been merged

Date	Description	Singular Vectors's characteristics						Forecast characteristics					
		HRES	VRES	OTI	Target area	EVO SVs	sampl	HRES	VRES	Tend	#	Mod Unc	Coupling
Dec 1992	**Oper Impl**	T21	L19	36h	globe	NO	simm	T63	L19	10d	33	NO	NO
Feb 1993	**SV LPO**	"	"	"	NHx	"	"	"	"	"	"	"	"
Aug 1994	**SV OTI**	"	"	48h	"	"	"	"	"	"	"	"	"
Mar 1995	**SV hor resol**	T42	"	"	"	"	"	"	"	"	"	"	"
Mar 1996	**NH+SH SV**	"	"	"	(NH+SH)x	"	"	"	"	"	"	"	"
Dec 1996	**resol/mem**	"	L31	"	"	"	"	TL159	L31	"	51	"	"
Mar 1998	**EVO SV**	"	"	"	"	YES	"	"	"	"	"	"	"
Oct 1998	**Stoch Ph**	"	"	"	"	"	"	"	"	"	"	YES	"
Oct 1999	**ver resol**	"	L40	"	"	"	"	"	L40	"	"	"	"
Nov 2000	**FC hor resol**	"	"	"	"	"	"	TL255	"	"	"	"	"
Jan 2002	**TC SVs**	"	"	"	(NH+SH)x+TC	"	"	"	"	"	"	"	"
Sep 2004	**sampling**	"	"	"	"	"	Gauss	"	"	"	"	"	"
Jun 2005	**rev sampl**	"	"	"	"	"	"	"	"	"	"	"	"
Feb 2006	**resolution**	"	L62	"	"	"	"	TL399	L62	"	"	"	"
Sep 2006	**VAREPS**	"	"	"	"	"	"	TL399(0-10)+TL255(10-15)	"	15d	"	"	"
Mar 2008	**VAREPS-mon**	T42	L62	48h	(NH+SH)x+TC	YES	Gauss	TL399(0-10)+TL255(10-15)	L62	15d/32d	51	YES	from d10

Outline

1. The rationale for a probabilistic approach to weather prediction
2. The ECMWF 32-day VAREPS/monthly ensemble system
3. Average performance of the ECMWF ensemble
4. Seamless probabilistic prediction:
   - Weekly-average predictions over Europe (March-April ’08)
   - Prediction of intense rainfall in Portugal and Spain (18-20 April ’08)
   - Prediction of cyclone Nargis (2-3 May 2008)

5. Future changes and conclusions

3. Trends in scores: ensemble RPSS, Z500 &T850 NH

The skill of the ensemble probabilistic predictions have been improving over the years, as it is illustrated by the ranked probability skill score (RPSS) for Z500 (left) and T850 (right) over Northern Hemisphere.

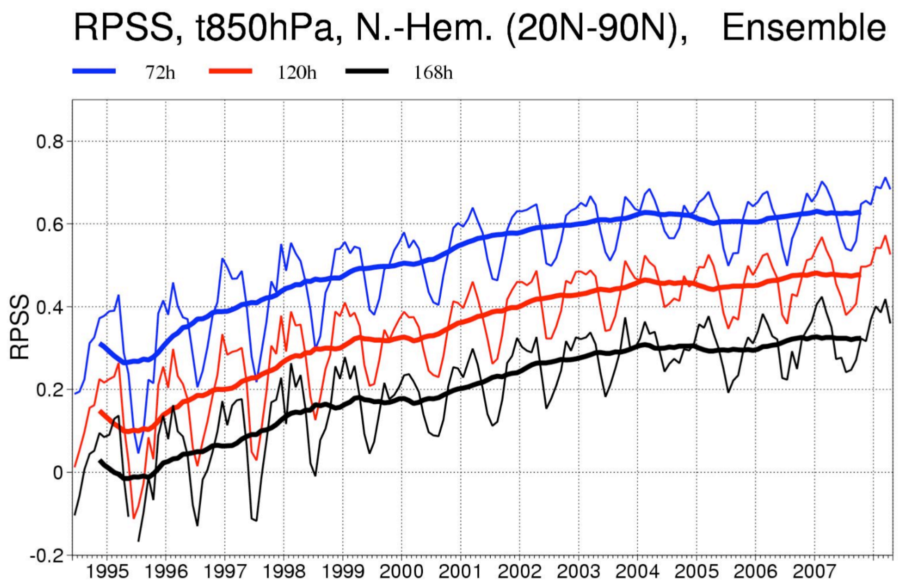

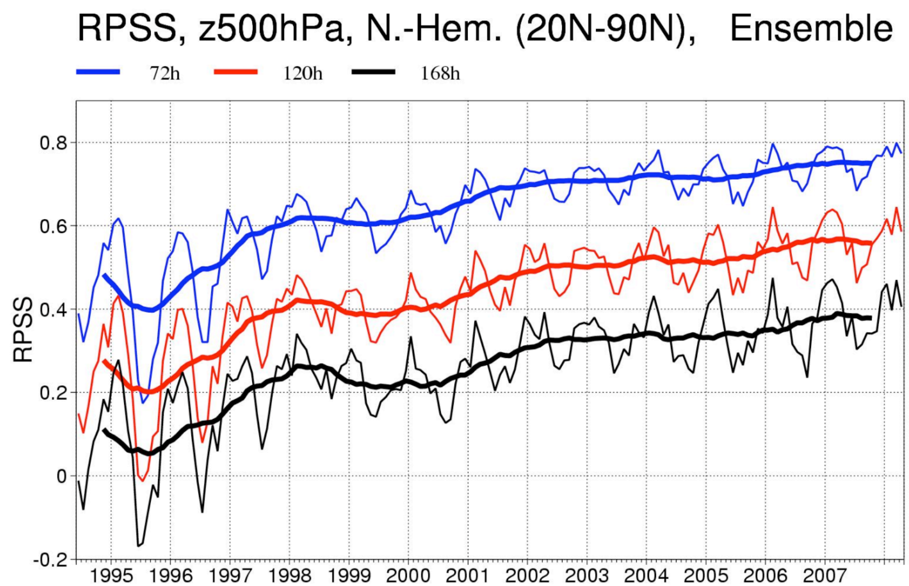

3. Trends in ensemble scores: RPSS Z500/T850 NH

The improvements in the accuracy of single and probabilistic forecasts can be measured in terms of the increase in lead time when a specified accuracy threshold is reached. These plots show the fc-time when the RPSS reaches a threshold that corresponds to the time the ACC of the HR forecast reaches 0.6 in 2006 (i.e. 0.301 for Z500 and 0.297 for T850). Results indicate for the EPS an increase in predictability in the past 10 years of ~ 2 days for Z500 and ~ 3 days for T850 over NH.

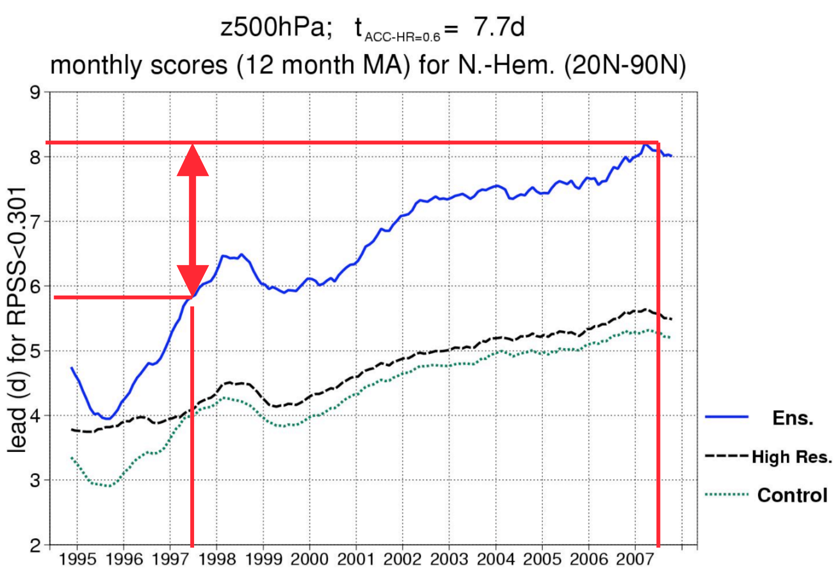

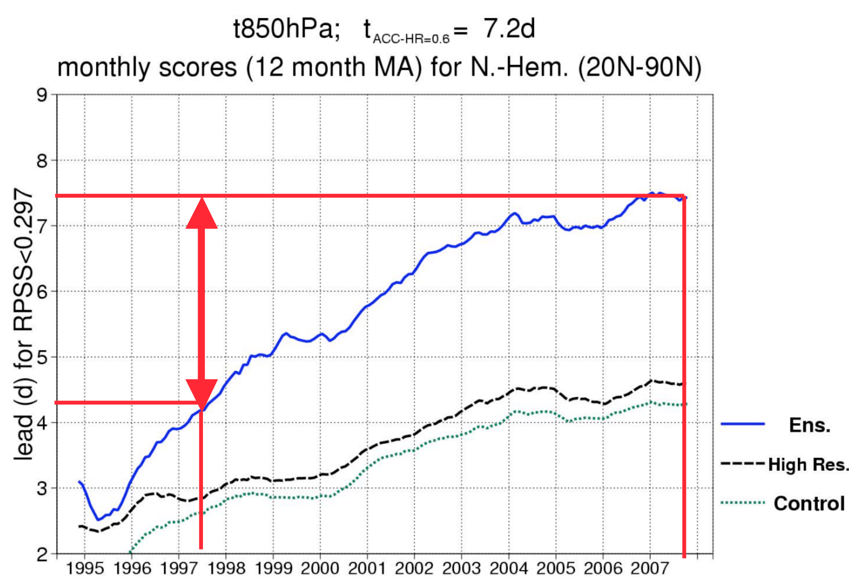

3. Monthly system: ROCA for PR(2mT>0.33c) NH

The monthly forecasting system has been running since 2005. Week-1 and week-2 probabilistic forecasts of some variables (e.g. 2m temperature anomalies) have been proven to be more skilful than climatological forecasts, or persistence. For some case, weekly probabilistic forecasts of accumulated precipitation has also shown to be skilful. Preliminary results have indicated that the new VAREPS/monthly system is in some cases even more accurate.

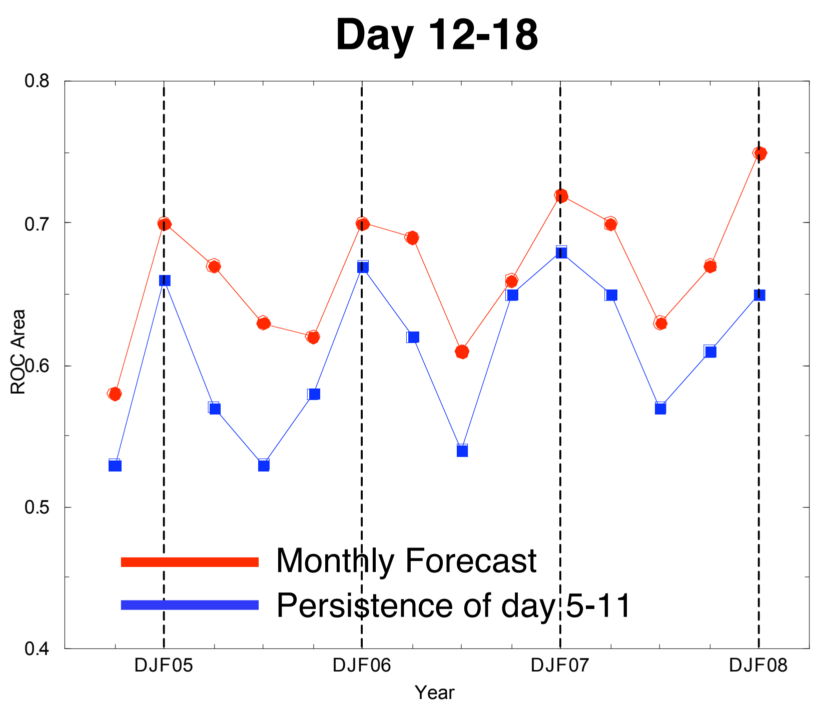

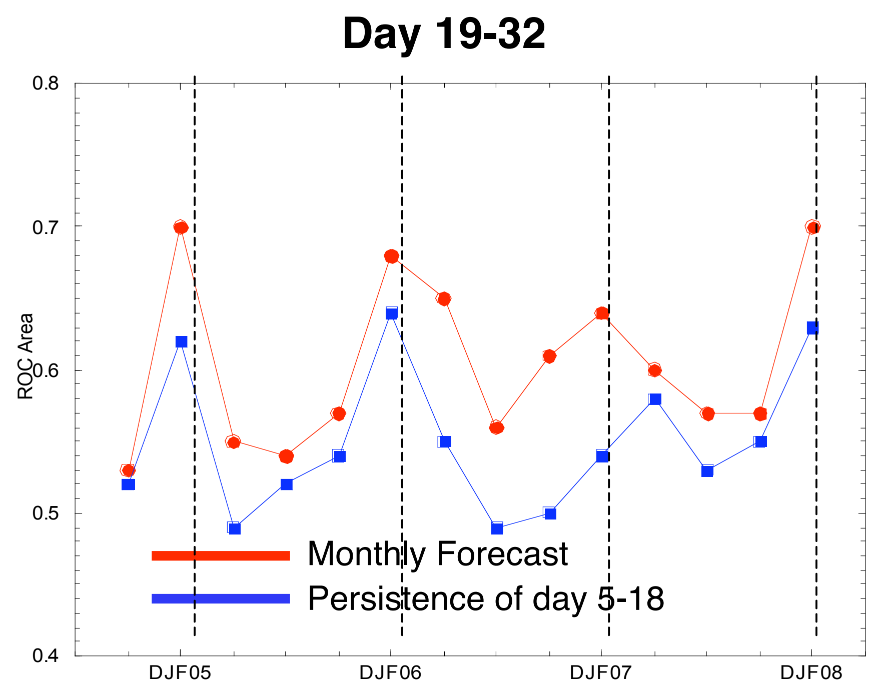

3. Performance of the TIGGE ensembles

The TIGGE data-base has given us the opportunity to assess the performance of almost all the operational global medium-range ensemble systems (that agreed to contribute to TIGGE). The following table lists the key characteristics of the ensembles compared in a a recent study (Park et al 2008).

Centre	Initial pert method (area)	Model error simul	Horizon res	Vert res	Fcst length (days)	# pert mem	#runs per day (UTC)	# mem per day	operation from*
BMRC(Australia)	SVs(NH,SH)	NO	TL119	19	10	32	2(00/12)	66	3 Sep 07
CMA (China)	BVs (globe)	NO	T213	31	10	14	2(00/12)	30	15 May 07
ECMWF	SVs (globe)	YES	TL399	62	0-10	50	2(00/12)	102	1 Oct 06
			TL255	62	10-15				
JMA (Japan)	BVs (NH+TR)+	NO	TL159	40+	9	50	1(12)	51	1 Oct 06
KMA(Korea)	BVs (NH)	NO	T213	40	10	16	2(00/12)	34	3 Oct 07
MSC(Canada)	EnKF (globe)	YES	TL149	28	16	20	2(00/12)	42	3 Oct 07
NCEP(USA)	BVs(globe)	NO	T126	28	16	20***	4(00/06/12/18)	84	5 Mar 07
UKMO(UK)	ETKF (globe)	YES	1.25x0.83deg	38	15	23	2(00/12)	48	1 Oct 06

3. ON07 (45c): Z500 STD over NH

This figure shows the ON07 average ensemble STD for Z500 over NH from Park et al (2008). The EC and the MSC ensembles have similar values. The NCEP ensemble has the lowest spread, while the CMA and JMA ensembles have the largest. The EC and BMRC ensembles have the smallest initial spread, and the fastest growth during the first 2 fc days.

This differences in ensemble spread strongly depend on the ensemble design (e.g. use of SVs) and model resolution/activity.

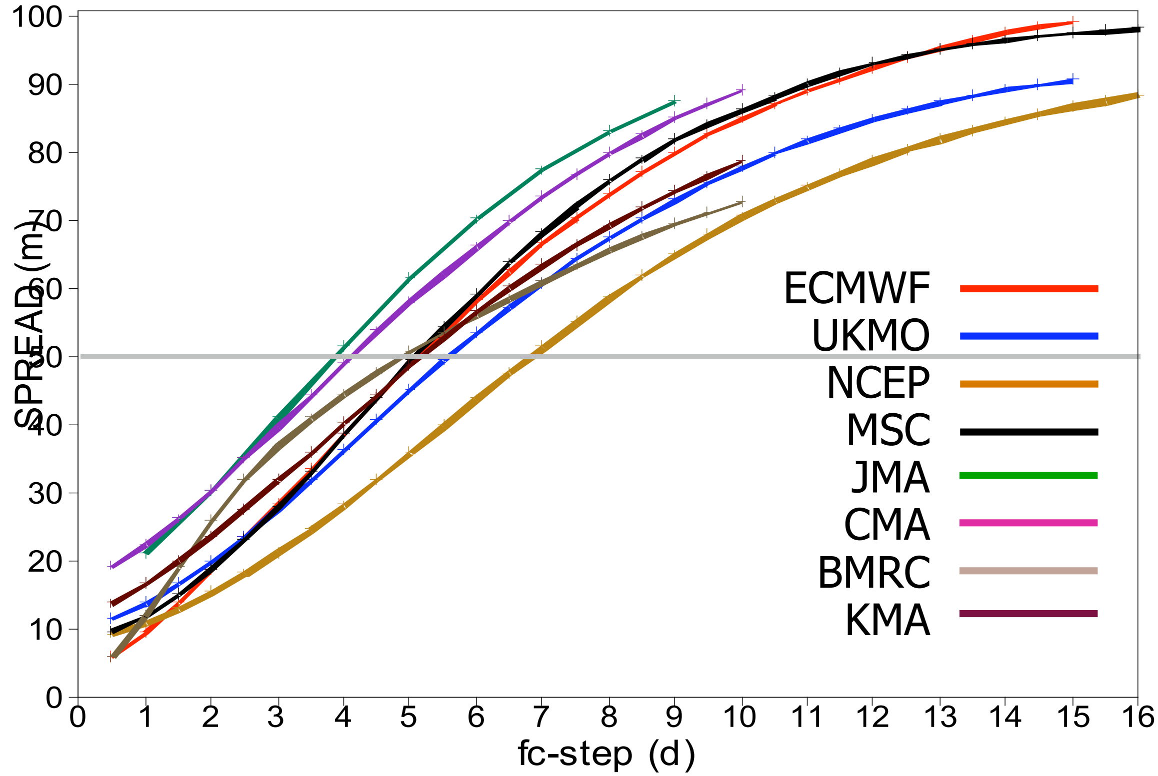

(from Park et al, 2008)

3. ON07 (45c): Z500 RMSE(EM) over NH

This figure shows the ON07 average RMSE of the ensemble-mean (EM) fc for Z500 over NH. The EC EM outperforms the group of 2nd best ensembles (MSC, NCAP, UKMO and JMA for this period) for the whole fc range, with ~0.75d gain in predictability at t+5d.

This indicates that the differences in skill of the ensemble probabilistic forecasts is not only due to model/analysis, but also to the ensemble design (e.g. use of SVs).

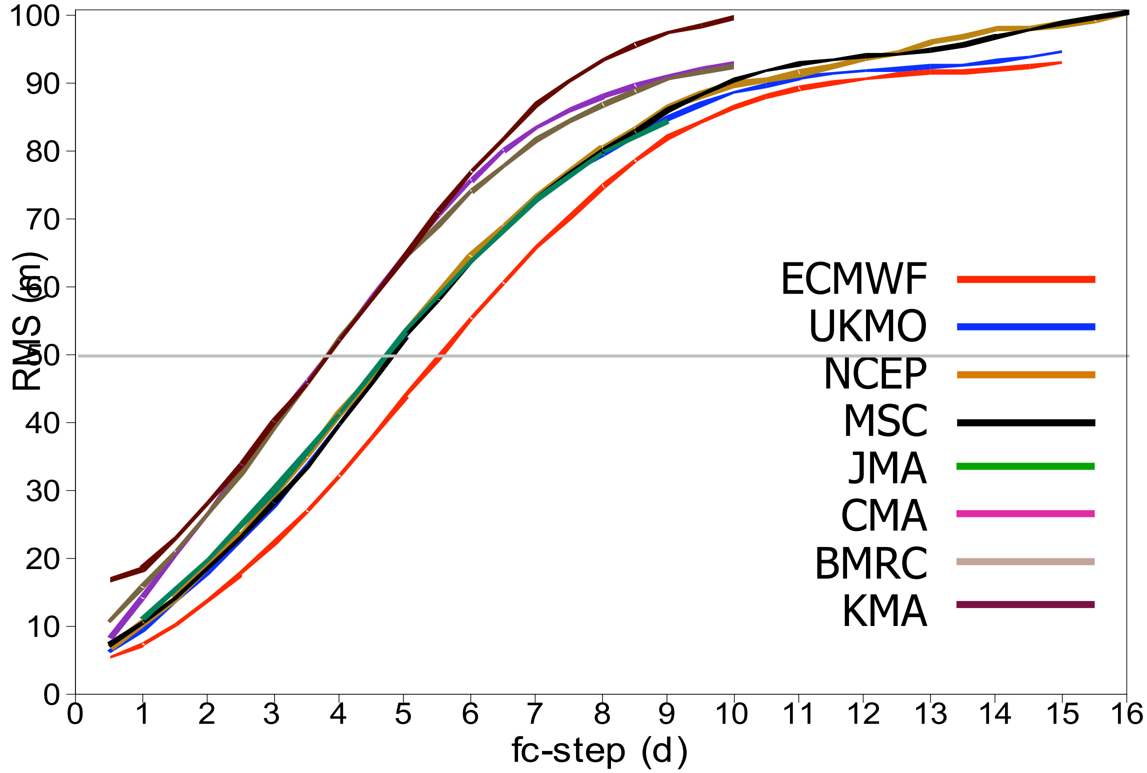

(from Park et al, 2008)

3. ON07 (45c): Z500 RPSS over NH

This figure shows the ON07 average RPSS of the ensemble fcs for Z500 positive anomalies over NH. The EC ensemble outperforms the group of 2nd best ensembles (UKMO, NCEP, MSC and JMA for this period) for the whole fc range, with ~1.0d gain in predictability at t+5d.

This also indicates that the differences in skill of the ensemble probabilistic forecasts is not only due to model/analysis, but also to the ensemble design (e.g. use of SVs).

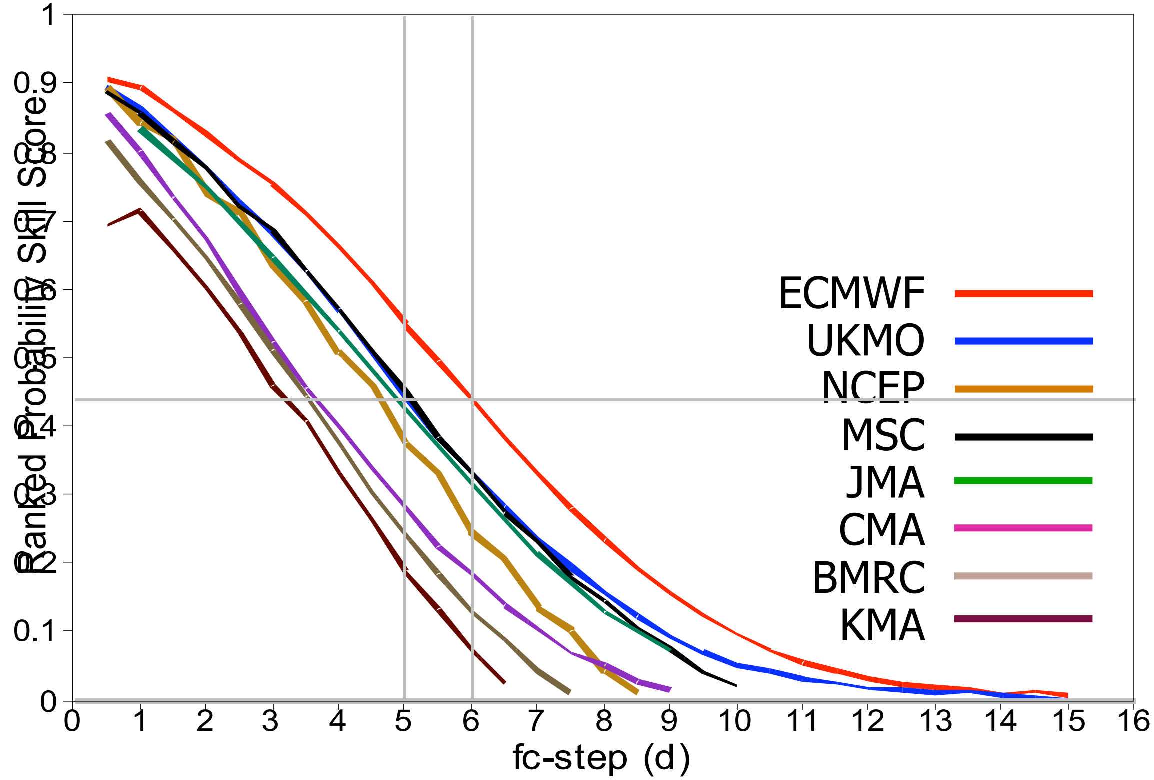

(from Park et al, 2008)

Outline

1. The rationale for a probabilistic approach to weather prediction
2. The ECMWF 32-day VAREPS/monthly ensemble system
3. Average performance of the ECMWF ensemble
4. Seamless probabilistic prediction:
    - Weekly-average predictions over Europe (March-April ’08)
    - Prediction of intense rainfall in Portugal and Spain (18-20 April ’08)
    - Prediction of cyclone Nargis (2-3 May 2008)
5. Future changes and conclusions

4. The advantage of a seamless probabilistic system

One of the advantages of having merged the 15-day and the monthly ensemble systems is that users have access to (seamless) probabilistic forecasts generated using the same model ranging from weeks to hours ahead:

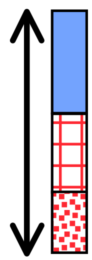

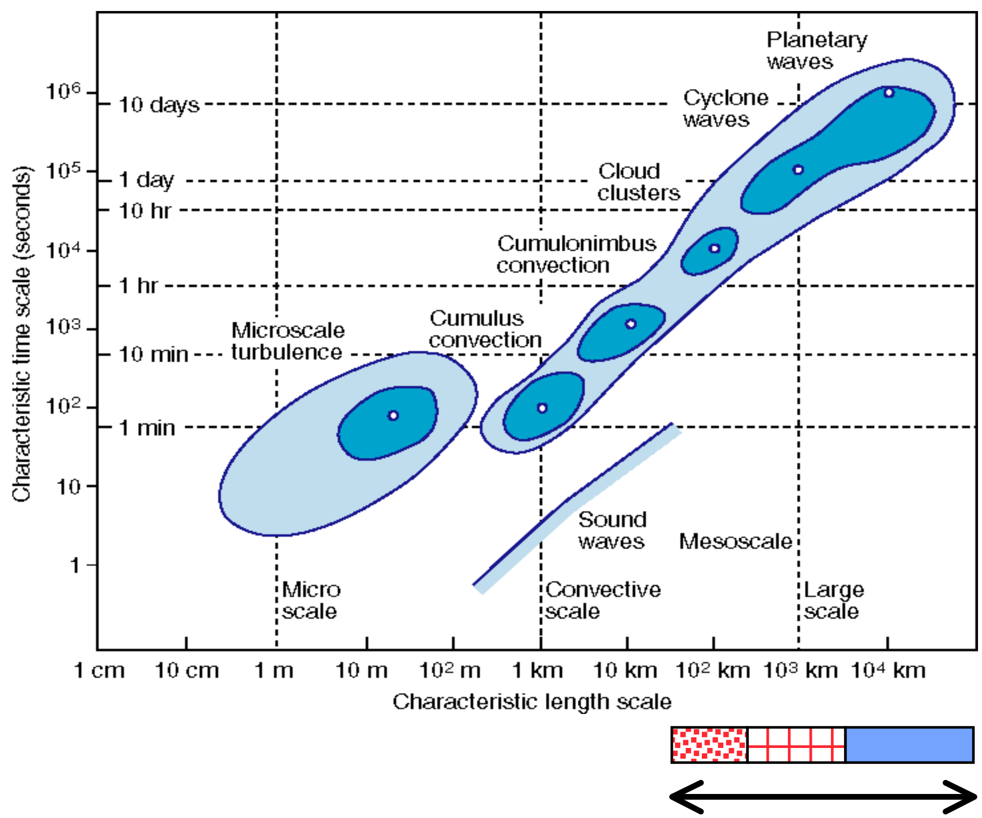

- In the long-range, weekly-average forecasts (of anomalies wrt model climate) can be used to predict large-scale weather patters.
- In the medium-range, daily probabilistic forecasts can be used to estimate more precisely the timing and location of future weather events.
- In the early forecast range (t<3d) hourly forecast (EPS-grams) can be used to predict in more details local weather conditions.

4.a-b From weekly to daily predictions

Seamless probabilistic forecasts from weeks to few hours ahead can be generated with the new ensemble system.

This is illustrated considering the wet period over Portugal and Spain between 14-20 April 2008, and in particular the intense precipitation of 18-19 and 19-20 April.

The forecasts used in the example are the operational ones available to the ECMWF Member States from the ECMWF web pages.

TP-anomaly 14-20 Apr

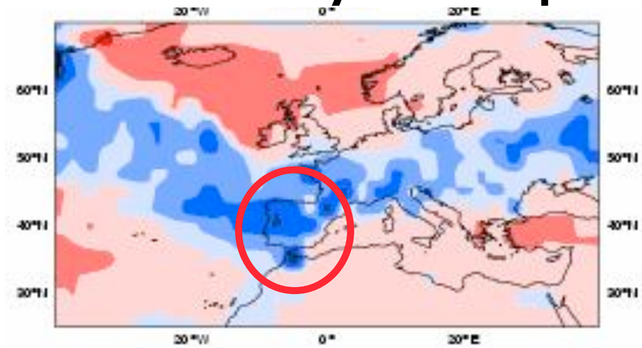

TP 18-19 Apr

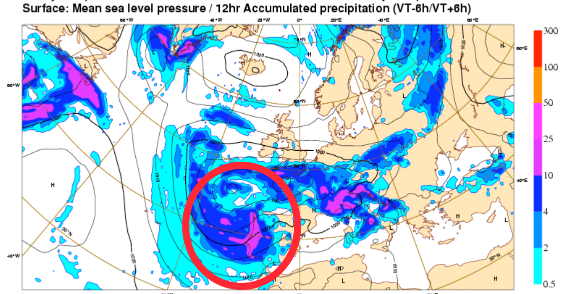

TP 19-20 Apr

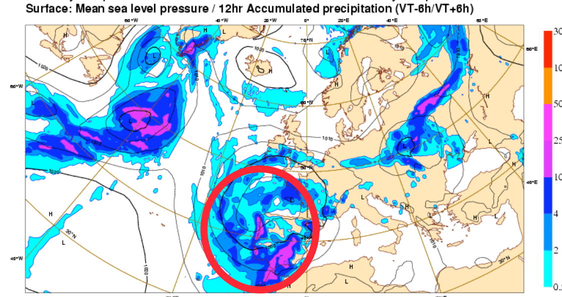

Observations	18-19 Apr	19-20 Apr
Lisbon	43mm	17mm
Gibraltar	17mm	16mm

4.a March-April 2008: week-1 and week-2 TP’ fcs

Week-1 (d5-11) average anomaly forecasts correctly predicted the transition to wet conditions over the Iberian peninsula and central Europe between the end of March and the beginning of April 2008. Week-2 (d12-18) average anomaly forecasts are less accurate, but in some cases gave the right signal.

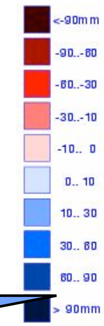

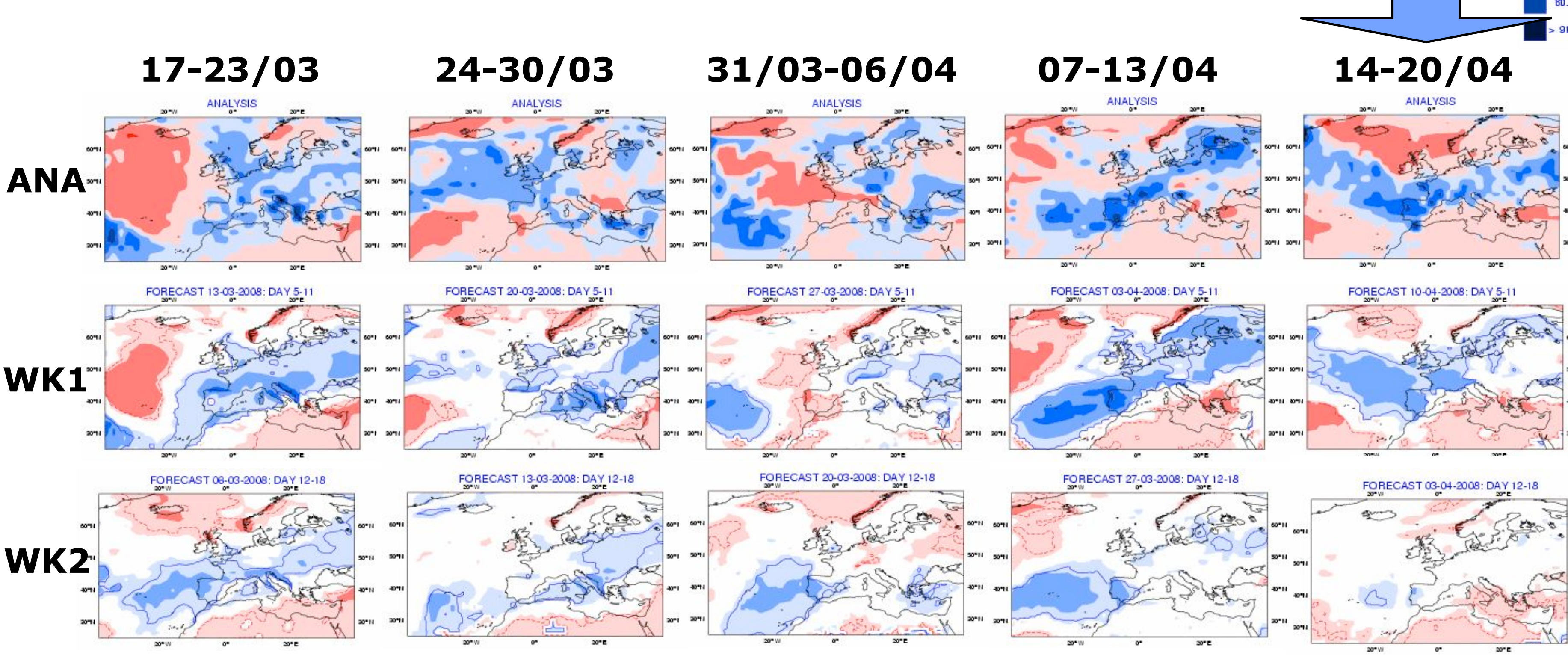

4.a March-April 2008: week-1 and week-2 2mT' fcs

Week-1 (d5-11) average 2m-temperature anomaly forecasts correctly predicted the areas of cold/warm anomalies between the end of March and the beginning of April 2008. Week-2 (d12-18) average anomaly forecasts are less accurate, but in some cases gave the right signal.

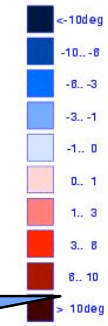

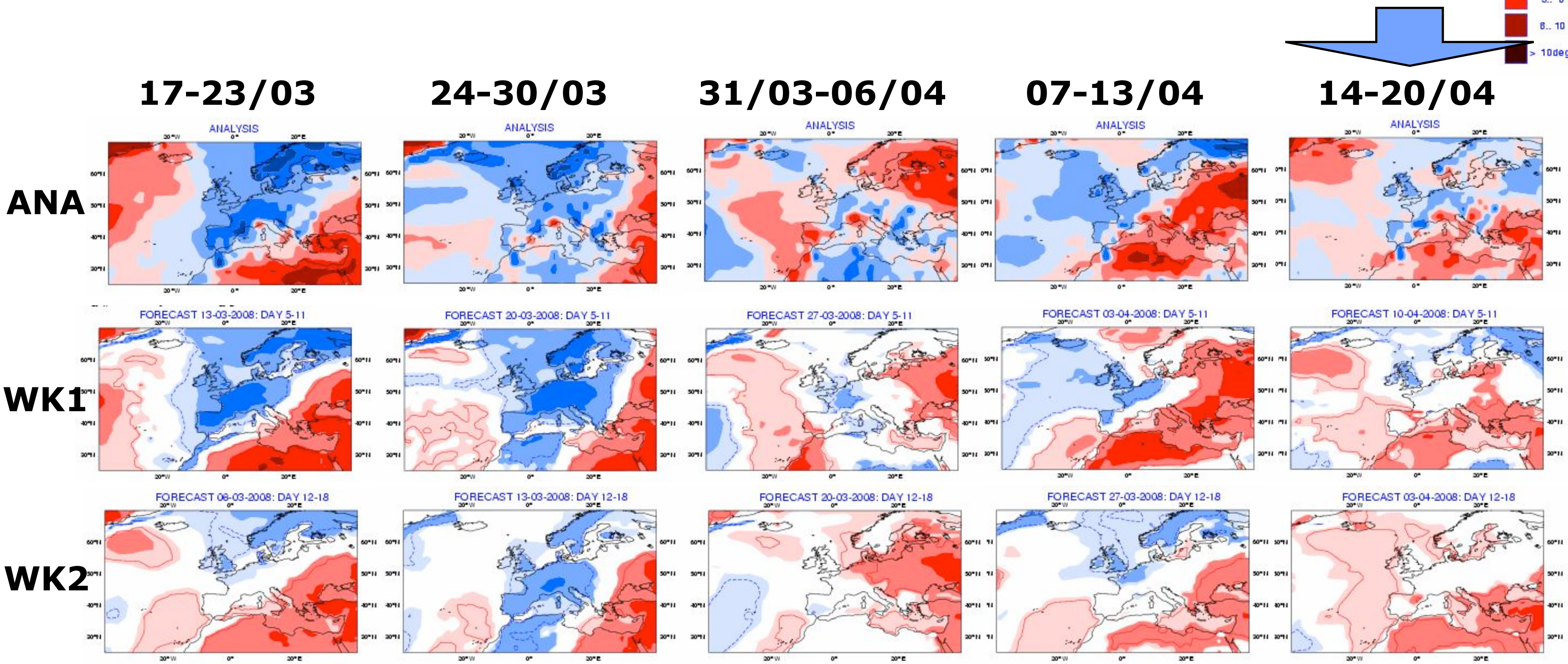

4.b Intense rainfall in Portugal and Spain on 18-20 April

Between the 18th and the 20th of April 2008, intense rainfall affected Portugal and Spain. The intense rainfall followed ~ 10 days of 'wetter than average' conditions.

Seamless probabilistic forecasts from weeks to few hours ahead can be generated with the new ensemble system.

- Did the VAREPS/monthly predictions of week-average states predict a 'wetter than normal' period? See discussion above (point 4.a)
- Did the VAREPS/monthly predictions of daily probabilities identify the period 18-20 April as a very wet period?
- Did the VAREPS/monthly predictions at a specific location (EPS-gram) correctly predict the rainfall amount?

4.b Daily prediction: PR fc for 18-19

Let’s focus on the forecasts for 18-19 April, and let’s see how the probabilities change as we get closer to the event.

These plots show the PR(TP>20mm/d) valid for 18-19 Apr and issued on 14 @12UTC (t+84/108) and on 15 @12UTC: PR(TP>20) fcs are consistent and increase for shorter fcs time.

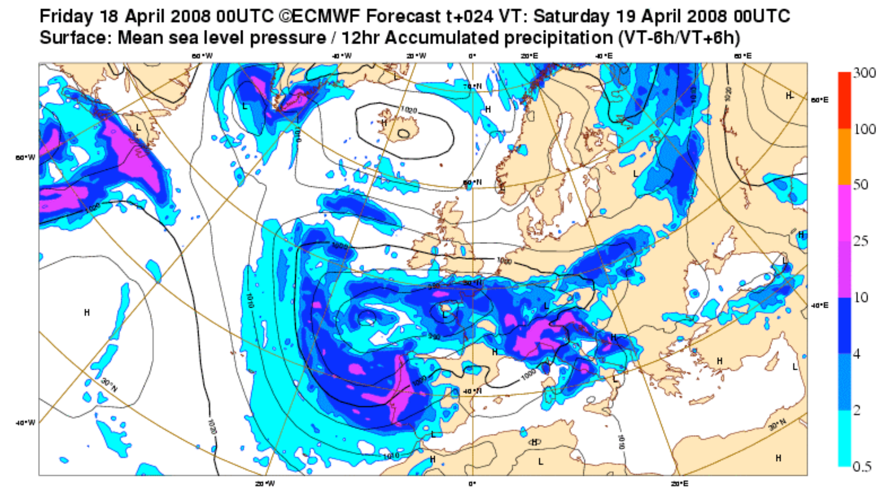

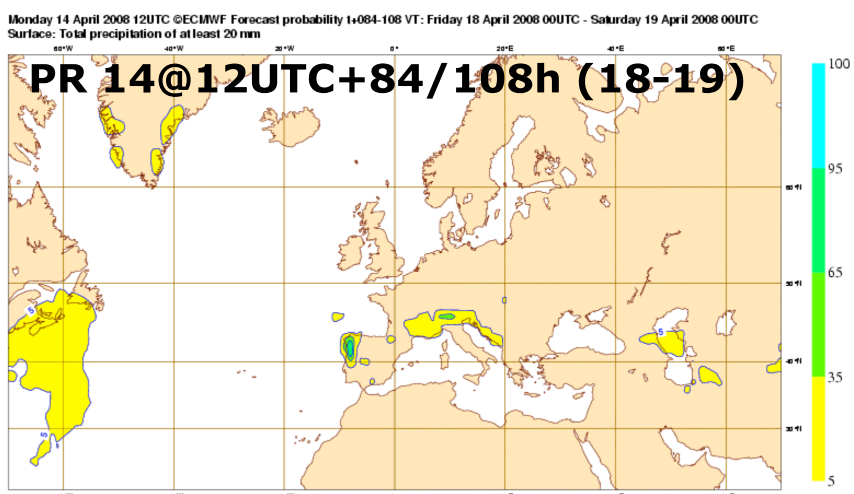

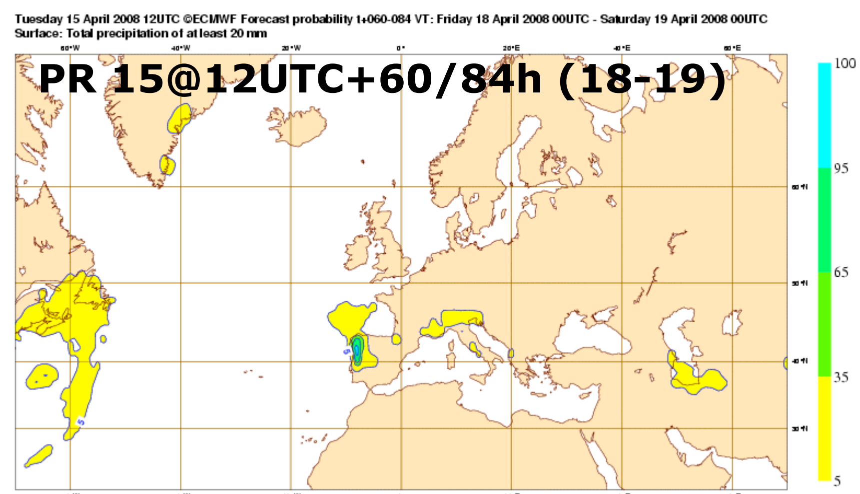

4.b Daily prediction: PR fc for 19-20

Let's focus on the forecasts for 19-20 April, and let's see how the probabilities change as we get closer to the event.

These plots show the PR(TP>20mm/d) valid for 19-20 Apr and issued on 15 @12UTC (t+84/108) and on 16 @12UTC: PR(TP>20) fcs are consistent and increase for shorter fcs time.

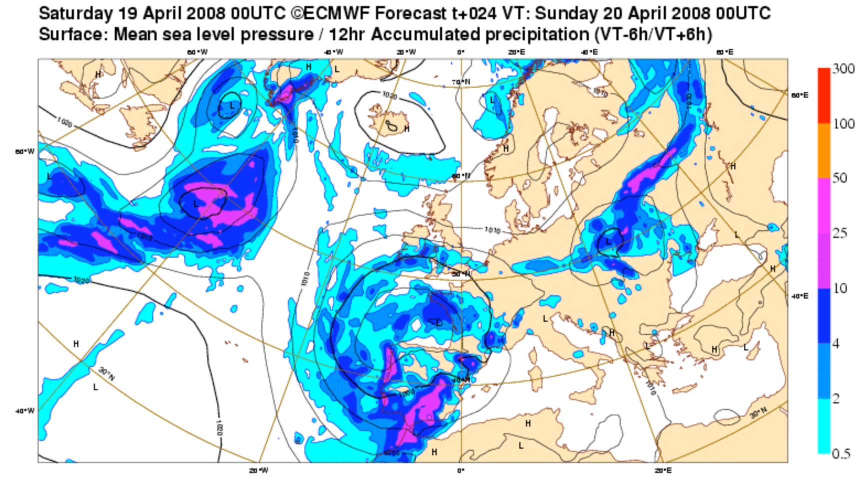

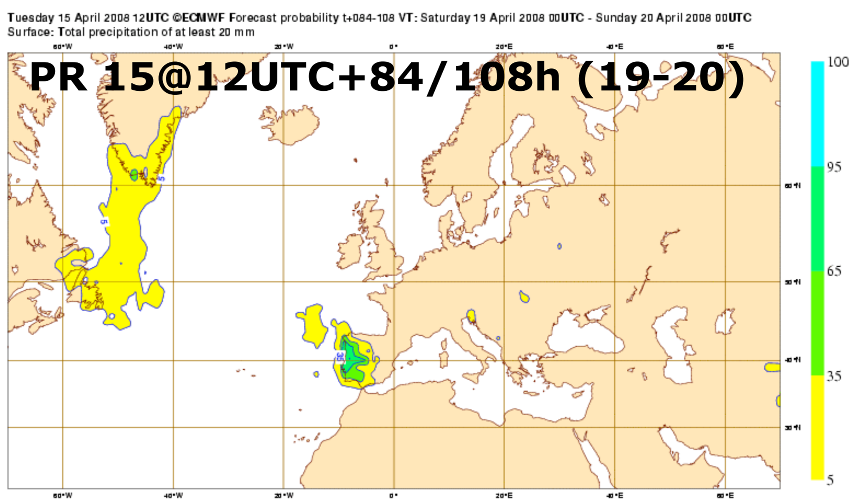

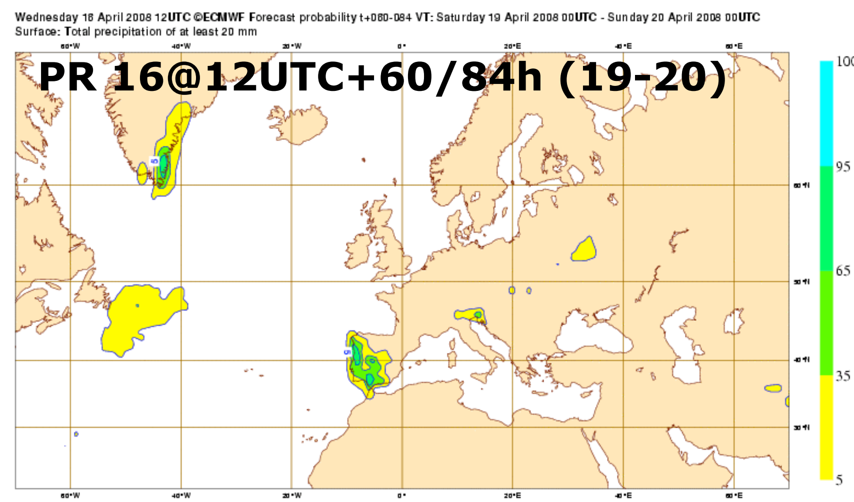

4.b Daily grid-point prediction: EPSgram Lisbon

EPS-grams for a single location can be used to make more localized weather forecasts.

These two plots show EPS-grams for Lisbon based on the ensemble forecasts started on 15 and 18 Apr @12UTC.

Between 06UTC of 18-19 (19-20) 43mm (17mm) of rainfall were observed.

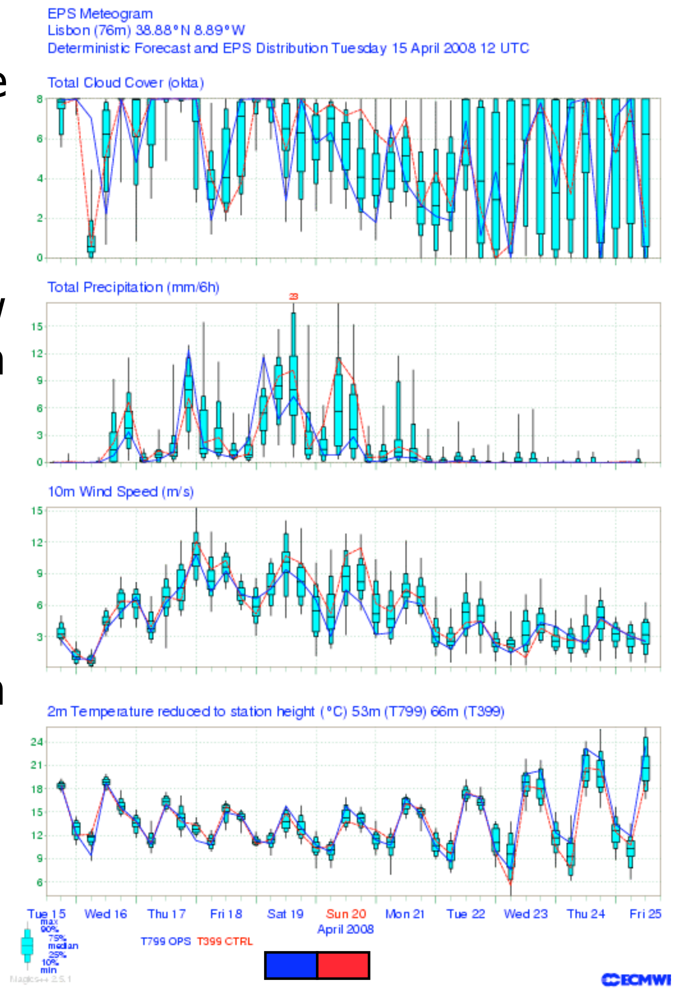

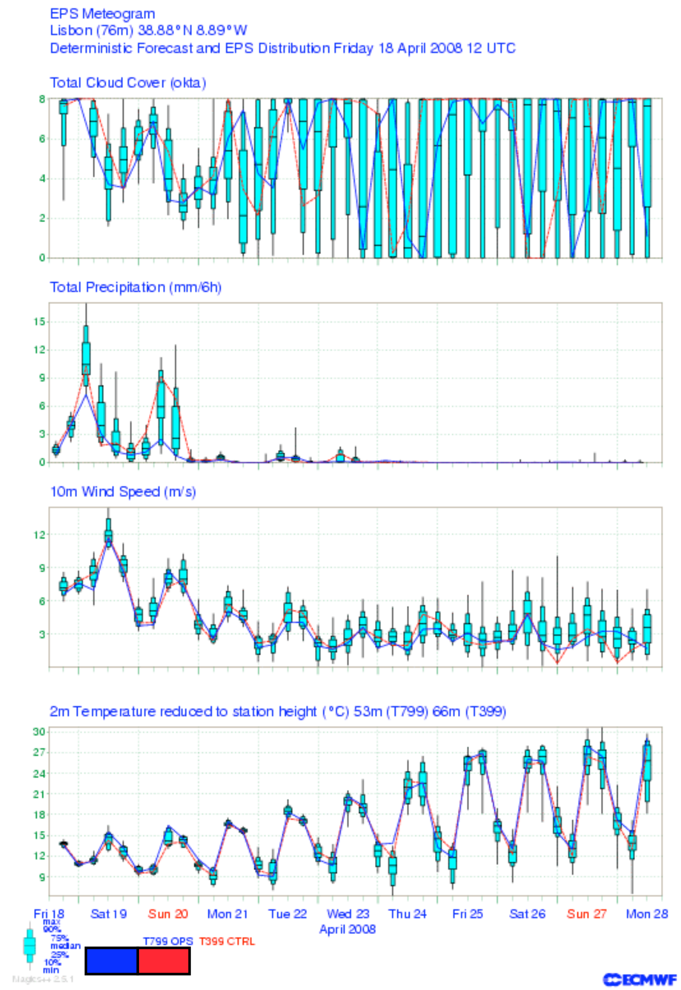

4.c Cyclone Nargis, 2-3 May 2008

On the 2nd and 3rd of May, cyclone Nargis hit Burma.

NASA satellite images demonstrate the scale of the impact. The top image was taken before the cyclone hit, with land and water features sharply defined. The lower image shows the aftermath on 5 May, with much of the Irrawaddy river delta region clearly flooded.

The UN estimates the death toll in the country could be 100,000 or more. Burma's state media says 28,458 died and 33,416 are missing.

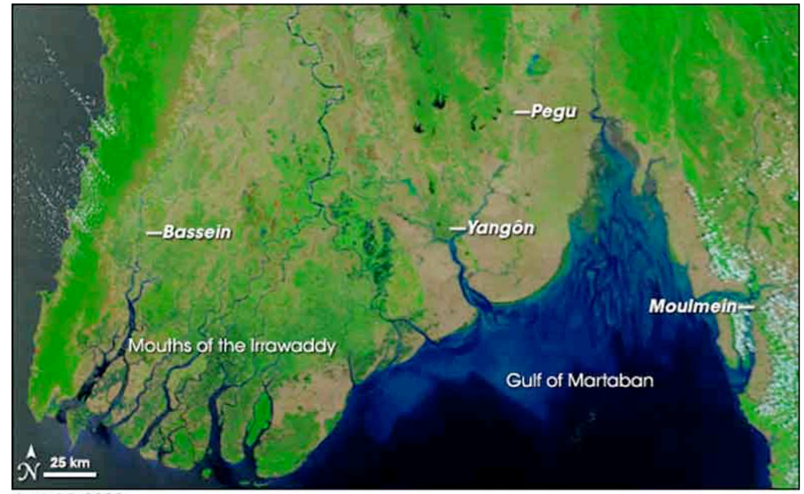

April 15, 2008

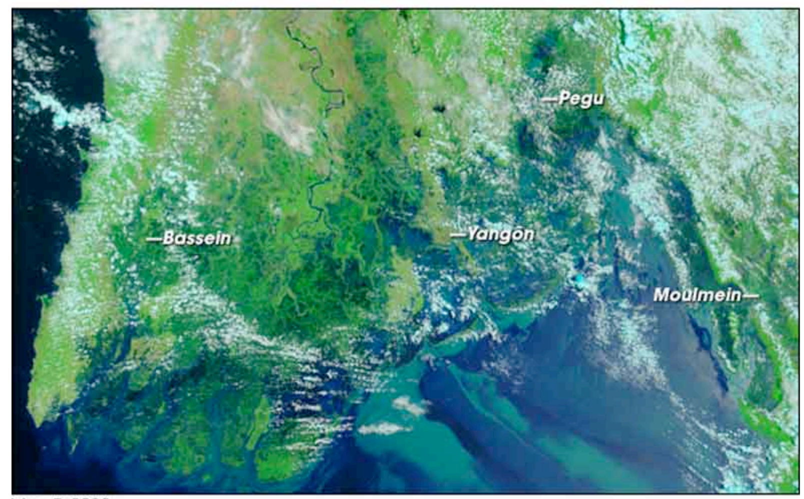

May 5, 2008

4.c Cyclone Nargis, 2-3 May 2008

It is interesting to point out that the ECMWF ensemble was predicting the genesis of a new TC few days before Nargis was observed, reported and named in the official bulletins.

These figures show the strike probability (i.e. the probability that a TC will pass within a 120km distance) predicted on 23 May (t+120-144h, left) and on 26 May (t+48-72h, right) valid for 29 May. The black dots shows the position of Nargis as reported in the TC bulletins between on 29 May.

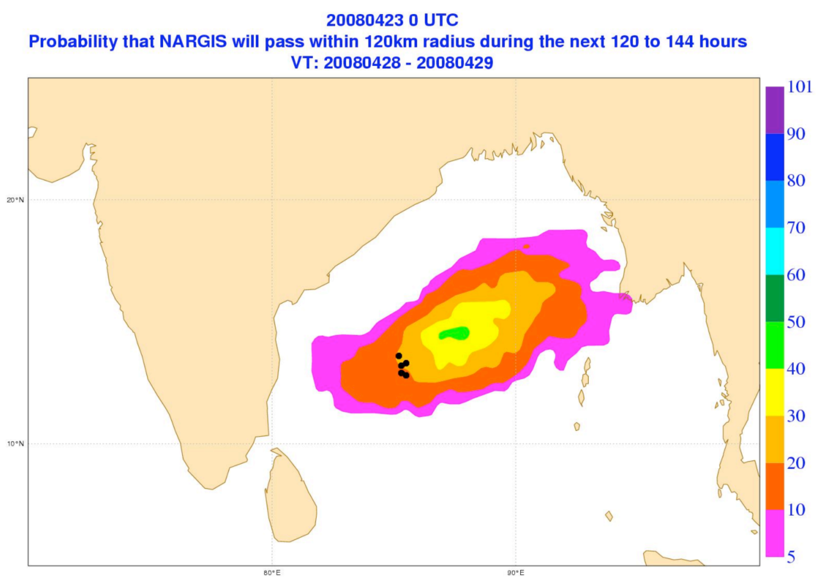

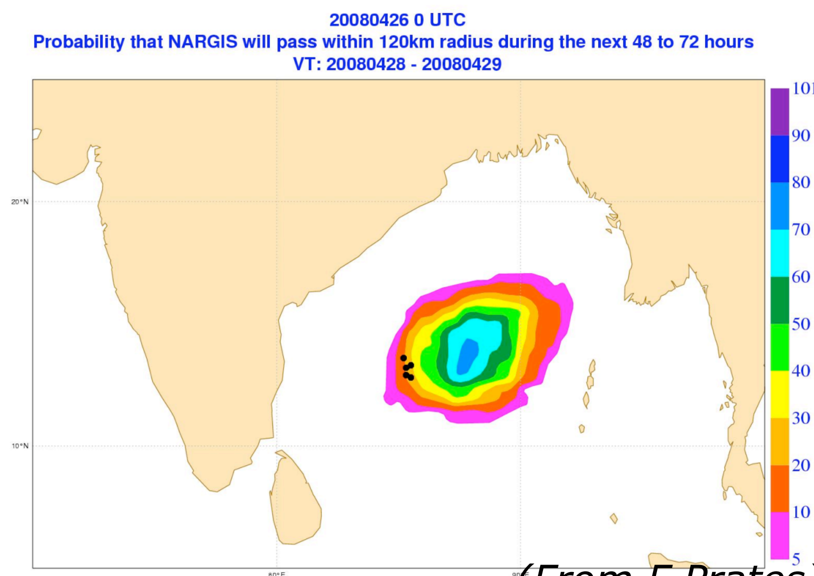

(From F Prates)

4.c Cyclone Nargis, 2-3 May 2008: strike probabilities

These figures show EPS strike probabilities (i.e. prob that the cyclone will pass within a 120km radius in the next 120h) issued on 27, 28 and 29 April @12.

Consecutive forecasts are consistent, with strike probabilities becoming narrower as time progresses.

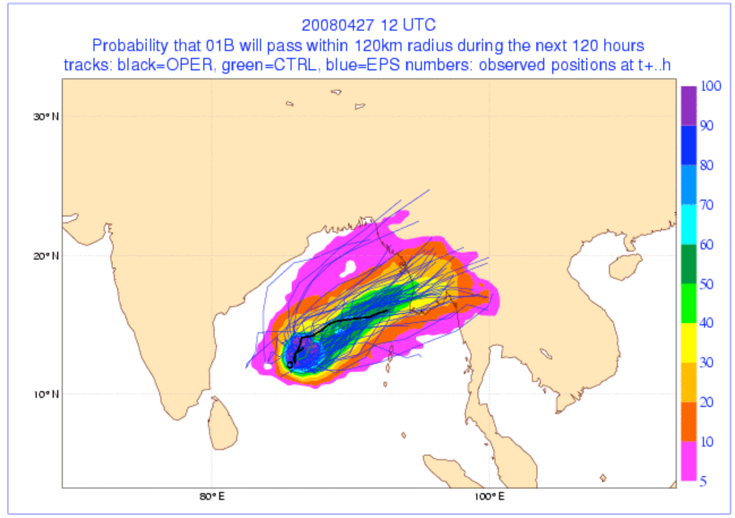

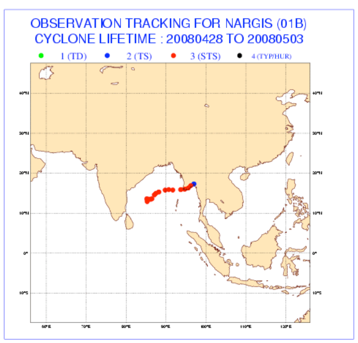

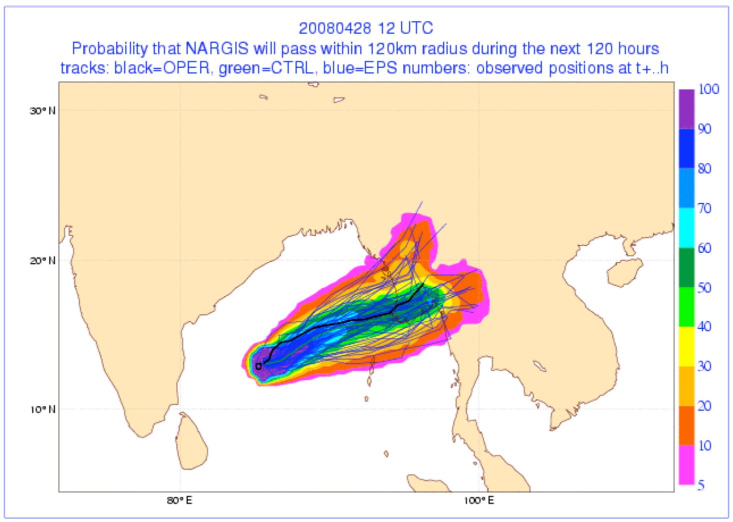

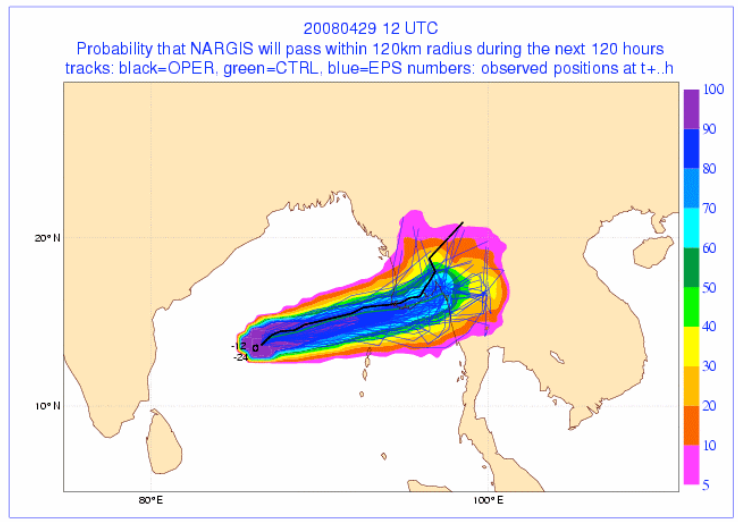

4.c Cyclone Nargis, 2-3 May 2008: Lagrangian EPSgram

These figures show Lagrangian EPS-grams for 10mWS and MSLP minimum issued on 27 and 29 April @12 for 2 May (left panel). Consecutive forecasts are consistent, with the EPS forecast range including the analyzed values.

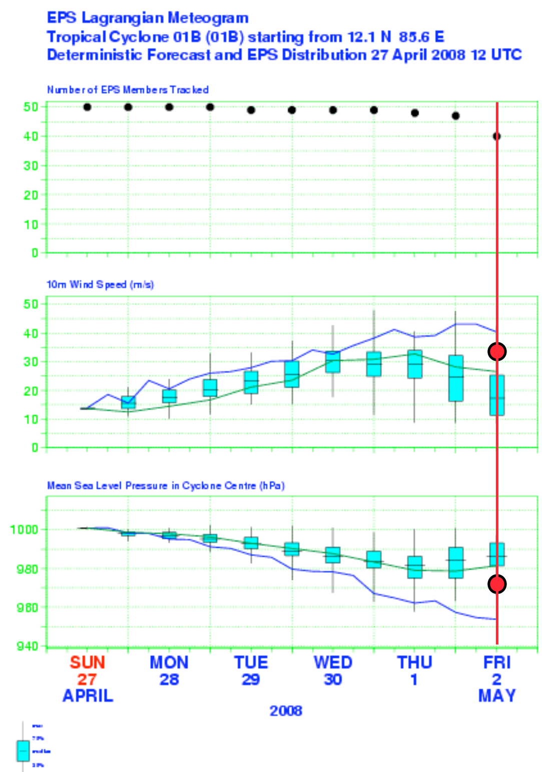

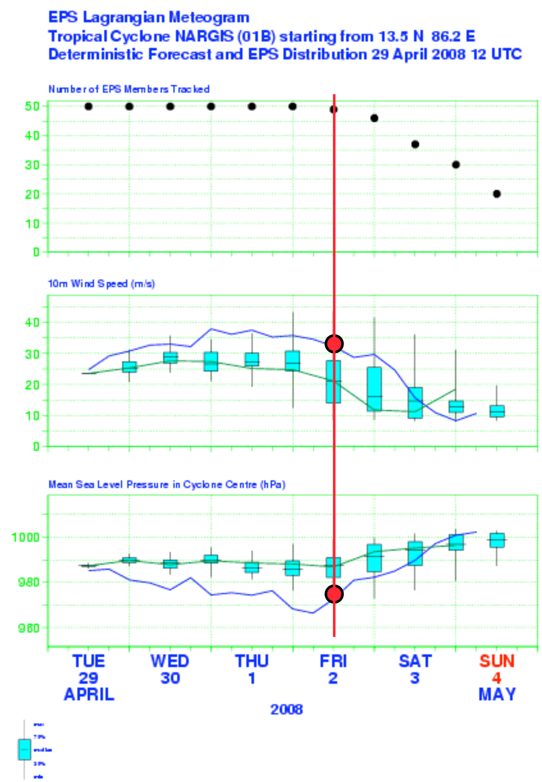

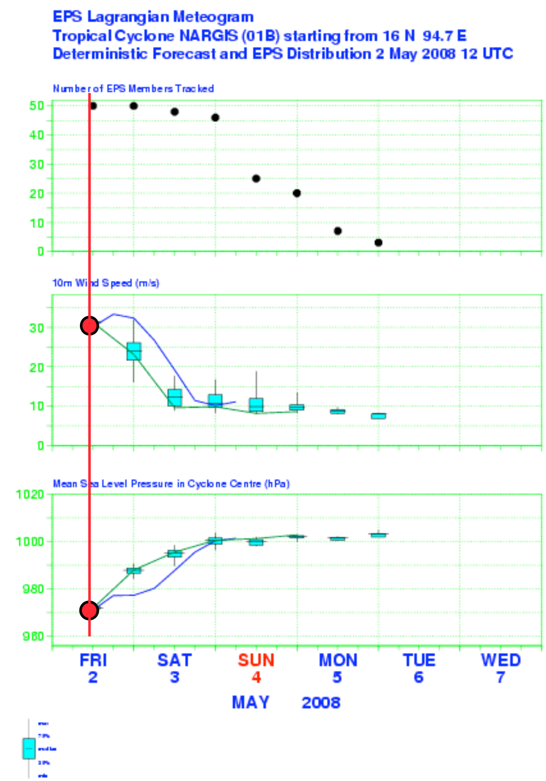

4.c Nargis EFI fcs: 27@12+108/132 for 10WS and TP

Another extremely valuable ensemble product that can be used to take the model climatology into account is the Extreme Forecast Index (EFI), which is generated comparing the EPS forecast cumulative distribution function with the model climatological cumulative distribution function.

These figures show t+108-to-132 EFI forecasts issued on 27 April @12 for 10m wind speed (top) and total precipitation (bottom).

Consistently with strike probabilities, EPS EFI maps for 10m wind speed (top) and total precipitation (bottom) predict extreme conditions over Burma.

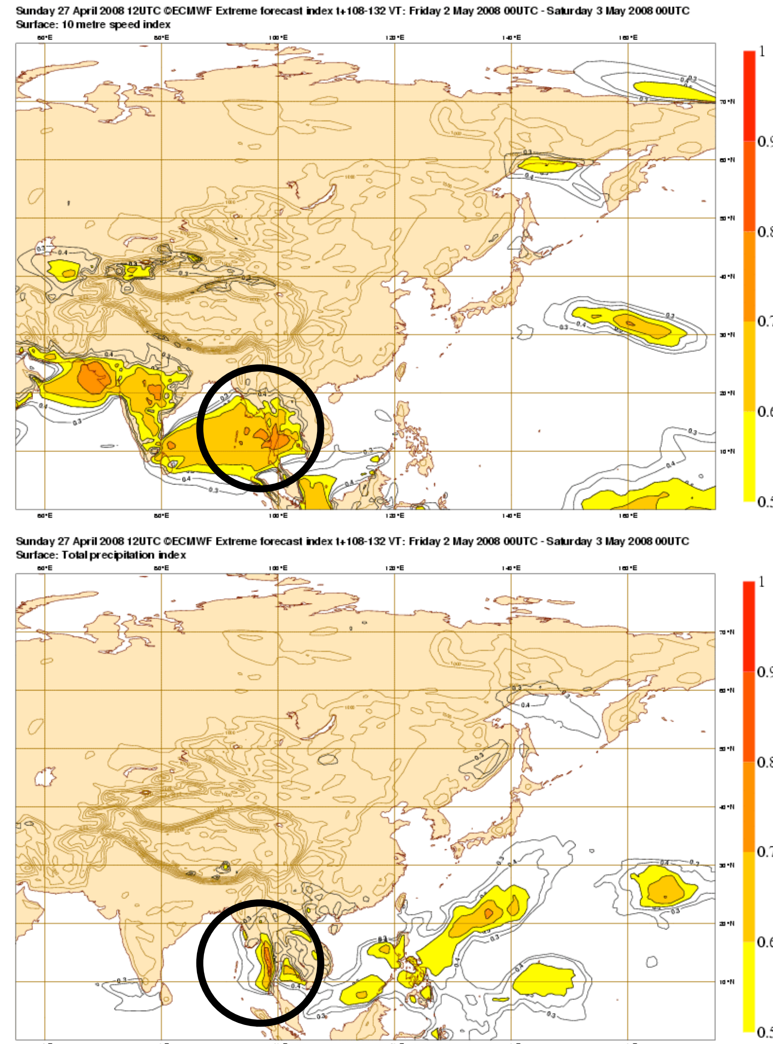

4.c Nargis EFI fcs: 29@12+60/84 for 10WS and TP

The EFI signal strengthen as the forecast time decreases, consistently with the strike probabilities getting narrower.

These figures show t+60-to-84 EFI forecasts issued on 29 April @12 for 10m wind speed (top) and total precipitation (bottom).

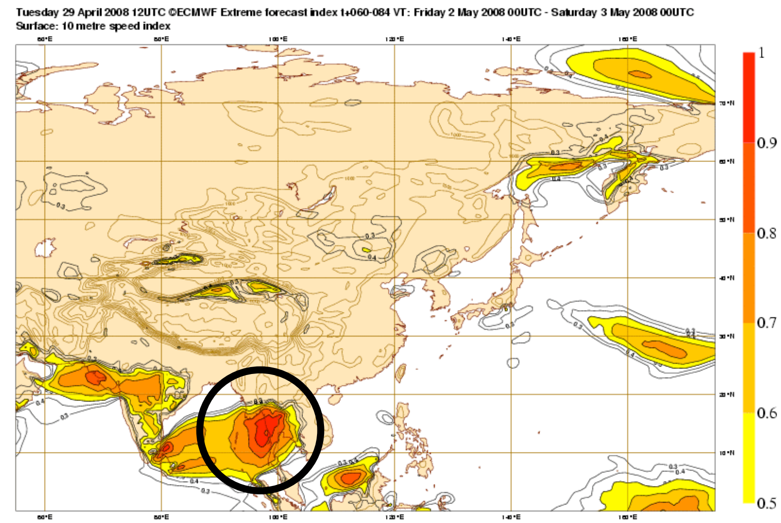

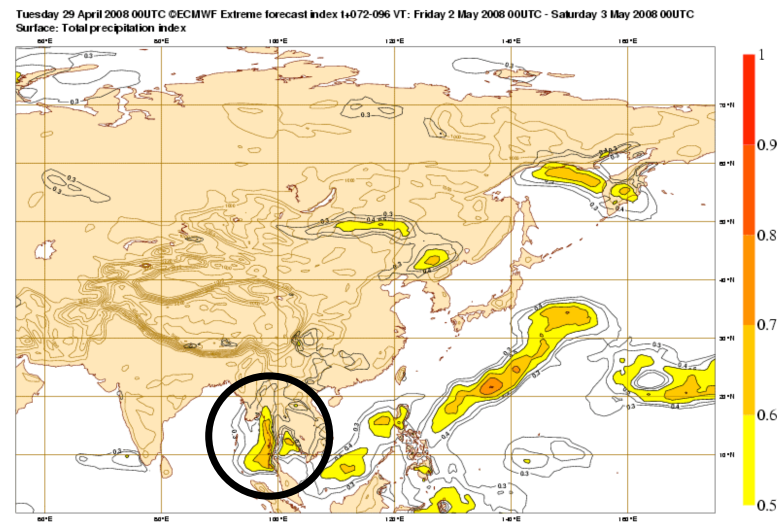

4.c Nargis: 2008-04-28@12+96h (VT 05-02@12)

This figure shows the SWH in the verifying analysis, and +96h fcs from the HRES (top-right) and EPS PR(SWH≥3m) and PR(SWH≥5m).

Contour interval is 1m for waves (top panels) and 2-5-10-25-50-75% for probabilities.

At this fc range the EPS predicts a 10-25% prob of SWH greater than 5 m.

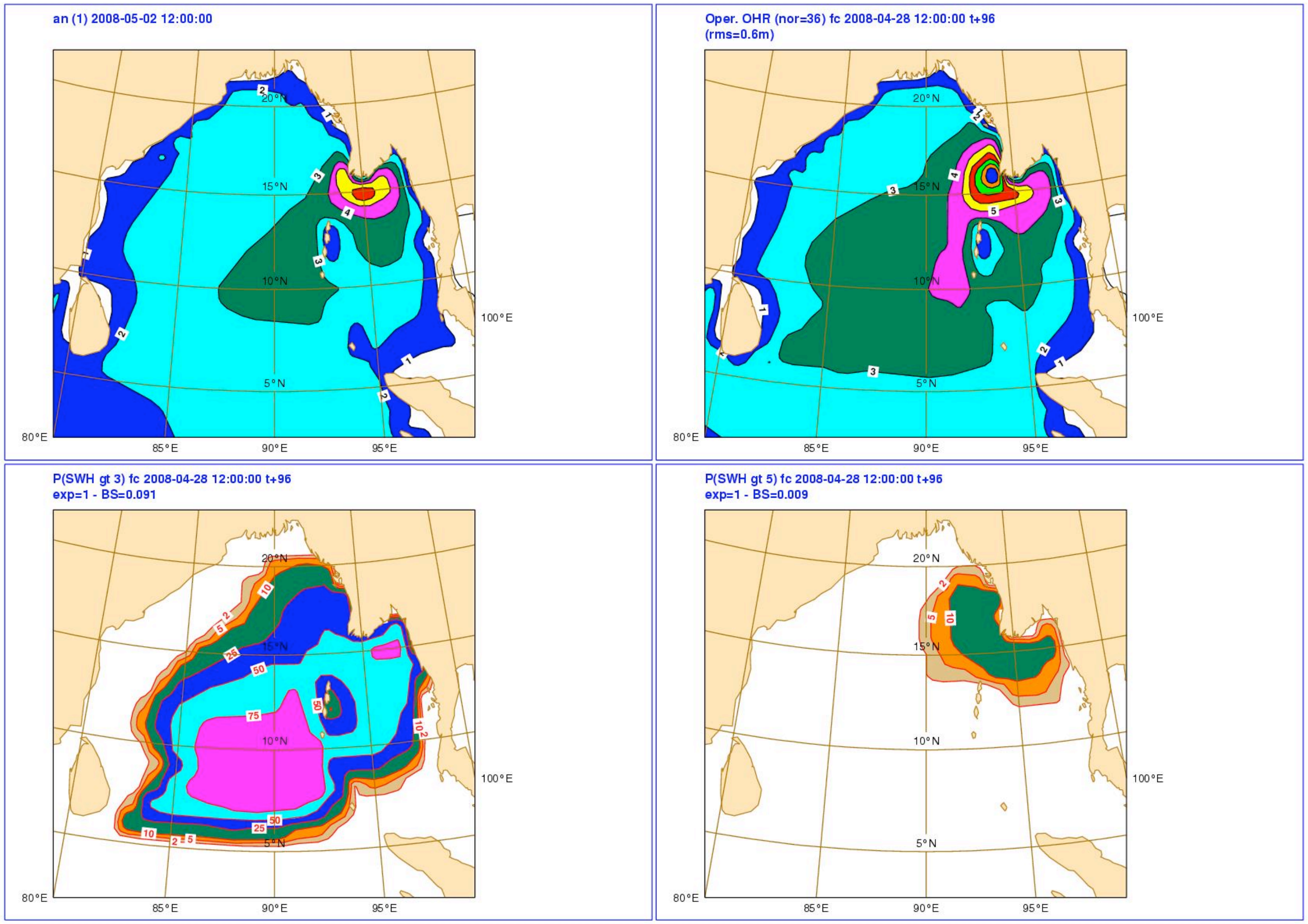

4.c Nargis: 2008-04-29@12+72h (VT 05-02@12)

This figure shows the SWH in the verifying analysis, and +72h fcs from the HRES (top-right and EPS PR(SWH≥3m) and PR(SWH≥5m).

Contour interval is 1m for waves (top panels) and 2-5-10-25-50-75% for probabilities.

At this fc range the EPS predicts a 25-50% prob of SWH greater than 5 m.

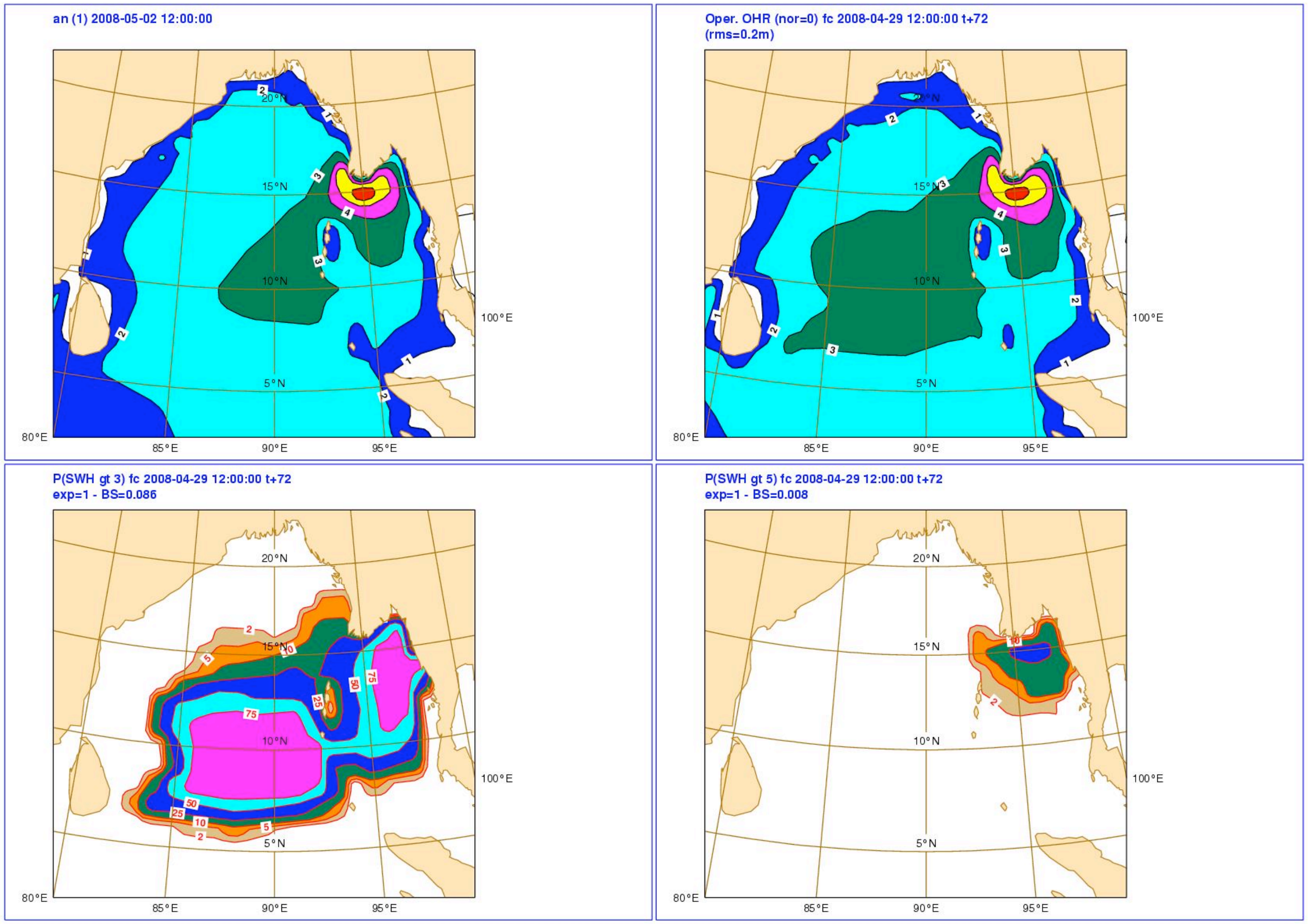

Outline

1. The rationale for a probabilistic approach to weather prediction
2. The ECMWF 32-day VAREPS/monthly ensemble system
3. Average performance of the ECMWF ensemble
4. Seamless probabilistic prediction:
    - Weekly-average predictions over Europe (March-April '08)
    - Prediction of intense rainfall in Portugal and Spain (18-20 April '08)
    - Prediction of cyclone Nargis (2-3 May 2008)

5. Future changes and conclusions

5. Ensemble Data Assimilation and Ensemble Prediction

This research aim to assess whether an ensemble of analyses can be used in the EPS to improve the sampling of initial uncertainties.

Experiments have been performed to test the use of an ensemble of analyses in the EPS in two possible ways:

• Using each analysis as a center around which to add SV-based perturbations *(fig 1)*

• Using the ensemble of analyses to generate a set of perturbations to be used in conjunction with SV-based perturbations, starting from either a reference analysis (e.g. the high-resolution unperturbed analysis), or the mean of the ensemble of analyses *(fig 2)*

This work may lead to the use of the ensemble of analyses instead of the evolved SVs in the EPS.

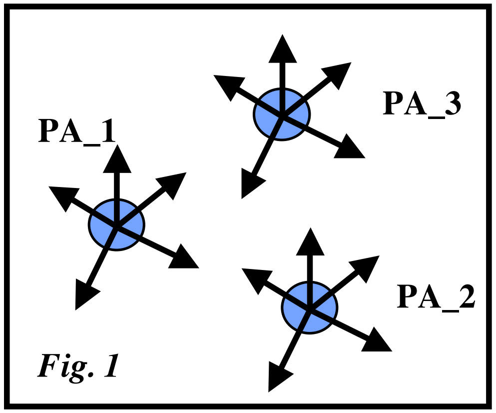

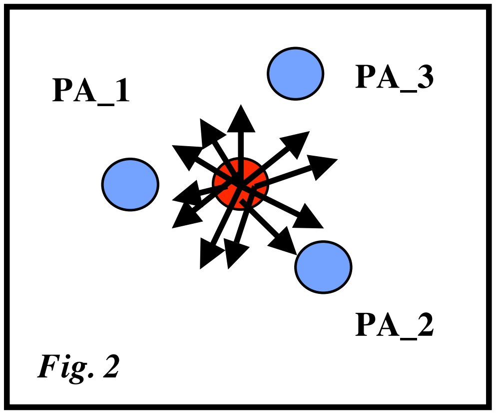

5. Ensemble Data Assimilation and Ensemble Prediction

The ensemble of analyses is run with random perturbations added to the observation and the SST. Differences between pairs of analyses (and forecast fields have the statistical characteristics of analysis and (forecast) error**.**

Work is in progress to assess the use of the ensemble of analyses to estimate the flow-dependent component of the background error (i.e. the "error of the day"), and to indicate where good data should be trusted in the analysis (yellow shading).

Work is also in progress to estimate the potential use of the ensemble of analyses in the ensemble system.

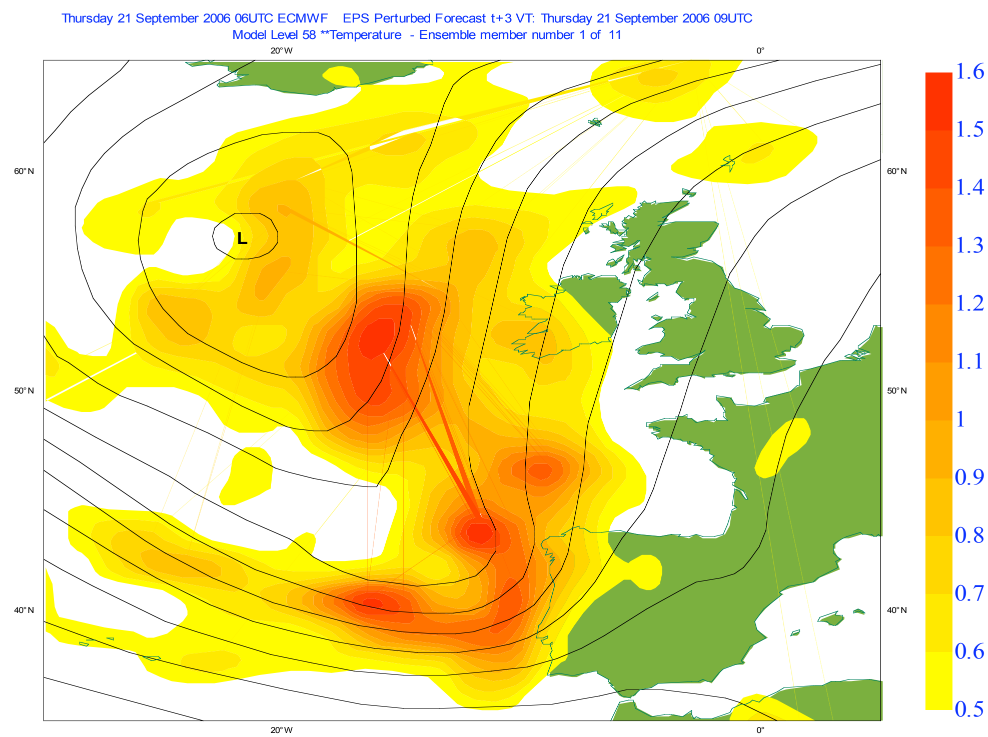

5. std of EDA, SVINI & EDA-SVINI at t=0 – 22/09/07

EDA-only initial perturbations (left panels) are smaller in amplitudes and in scale than SVINI perturbations (middle panels), but are geographically more global.

The right panels show the effect of using both EDA and SVINI perturbations.

EDA **SVINI** **EDA-SVINI**

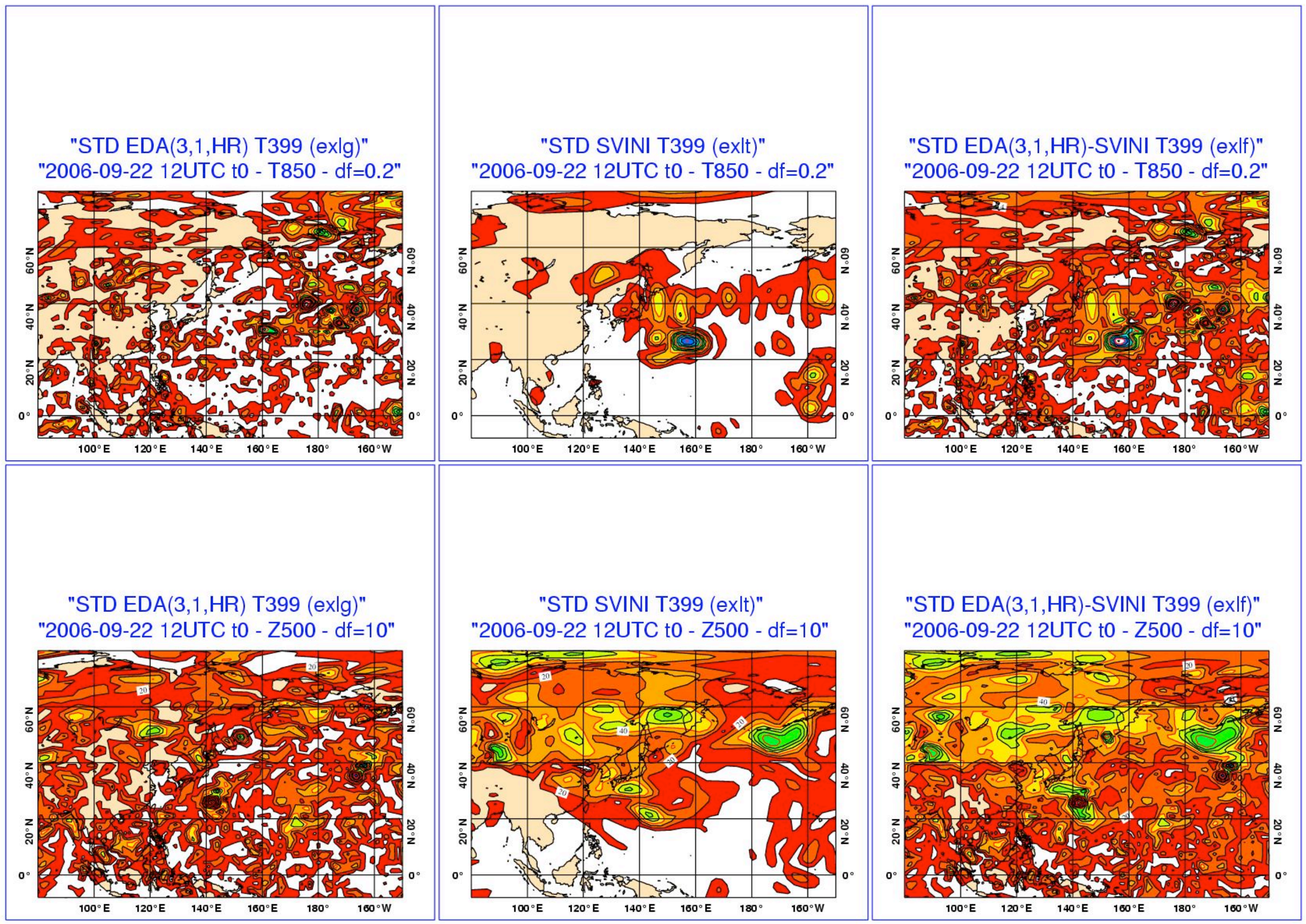

5. (MEM5-CON) SVINI EPS - 22/09/2007 t=0

At t=0, SVINI perturbations (defined by a combination of initial SVs) tend to be localized in space, and to have a larger component in potential than kinetic energy. They also show a westward tilt with high, typical of baroclinically unstable structures.

This figure shows two vertical cross sections of the temperature and zonal-wind components of the MEM5 perturbation.

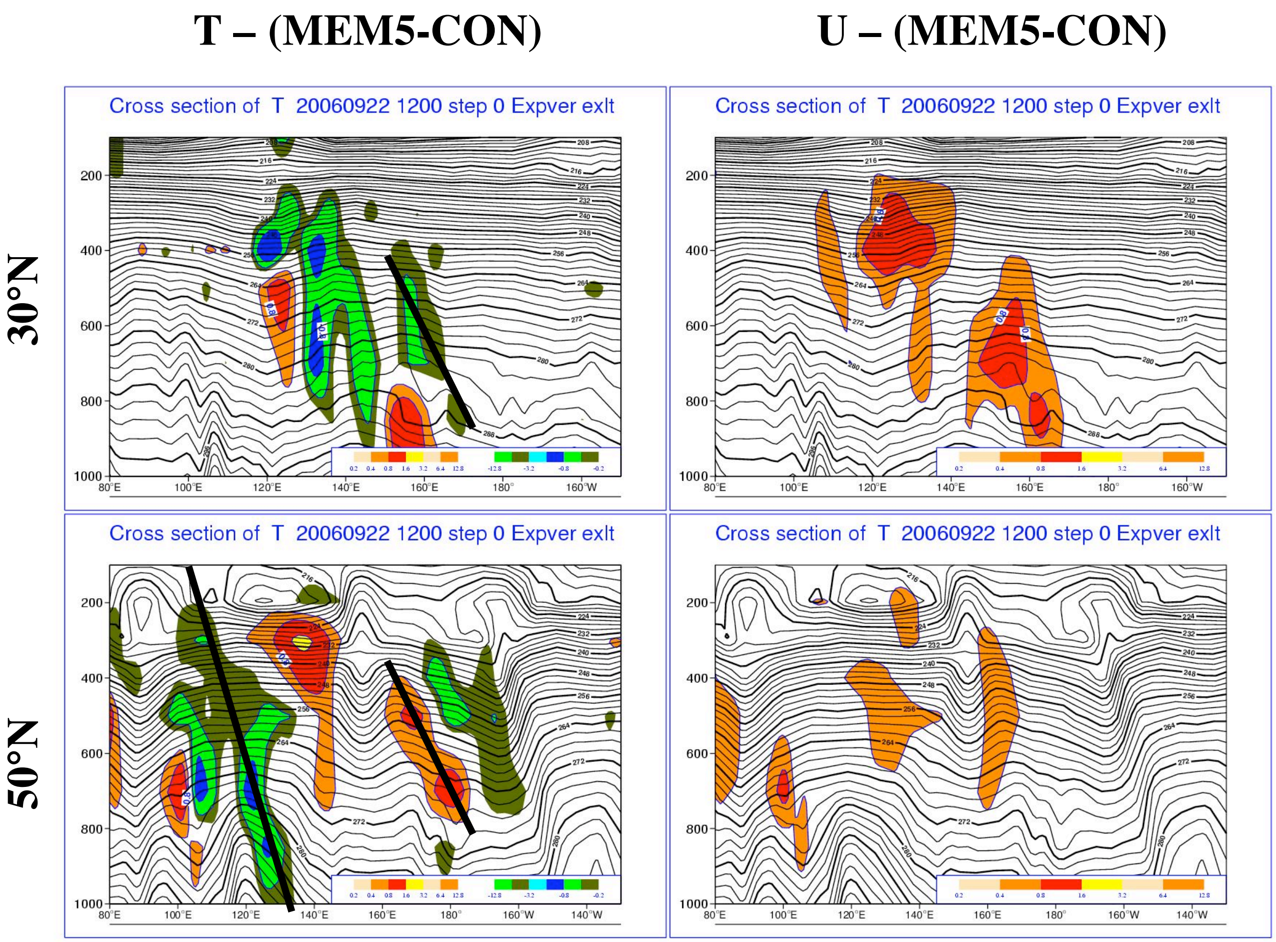

5. (MEM5-CON) EDA EPS - 22/09/2007 t=0

At t=0, EDA perturbations have a smaller scale than the SVINI perturbations, and are less localized in space. They have a similar amplitude in potential and kinetic energy. They tend to have more a barotropic than a baroclinic structure.

This figure shows two vertical cross sections of the temperature and zonal-wind components of the MEM5 perturbation.

T – (MEM5-CON) **U – (MEM5-CON)**

30°N

50°N

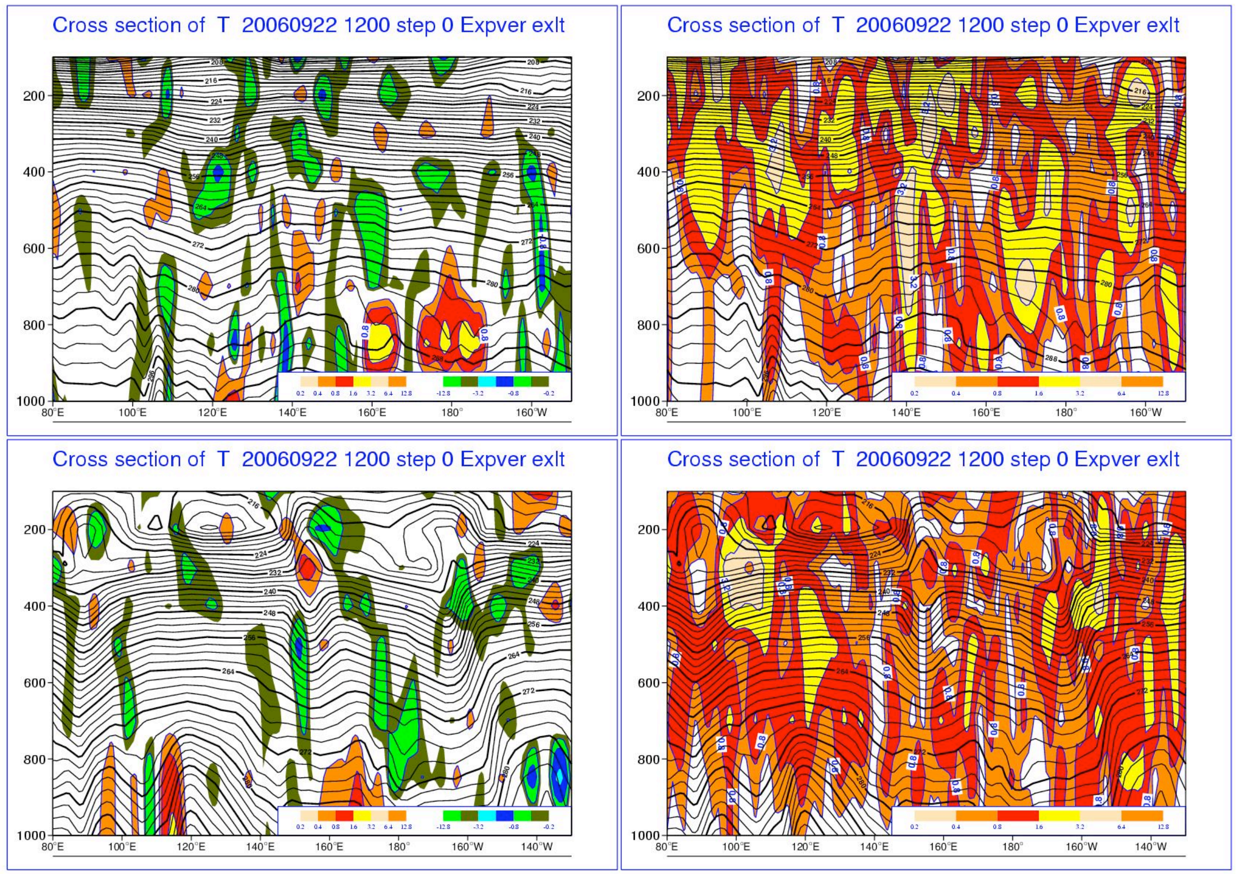

5. std/EM of EDA, SVINI, EDA-SVINI & SVEVO-INI EPS

The EDA-SVINI ensemble combines the benefits of the EDA and the SV techniques. Over both the NH (left) and the tropics (right), the EDA-SVINI ensemble has a better tuned spread, and the smallest ensemble-mean error (in terms of T850). In the extra-tropics, compared to the SVINI the EDA ensemble severely underestimates the spread, but over the tropics the EDA ensemble has initially a larger spread.

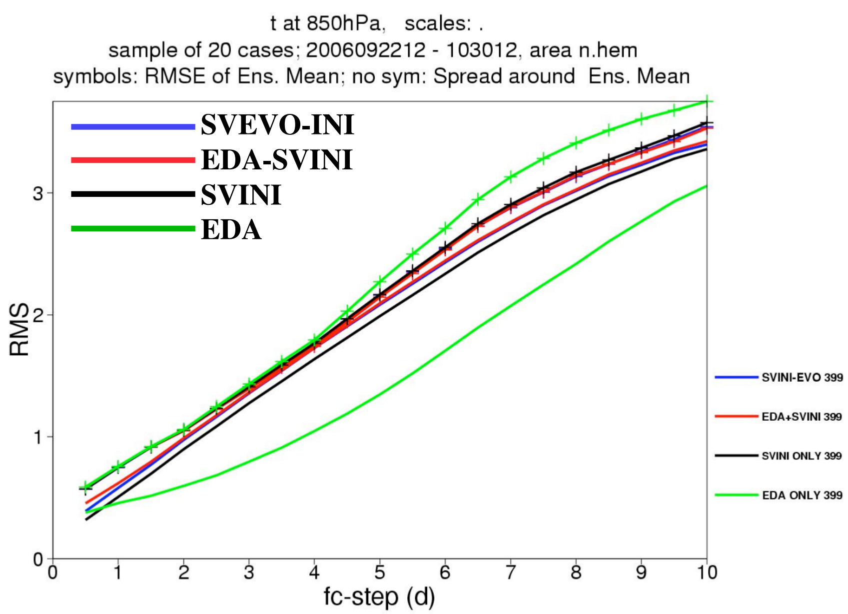

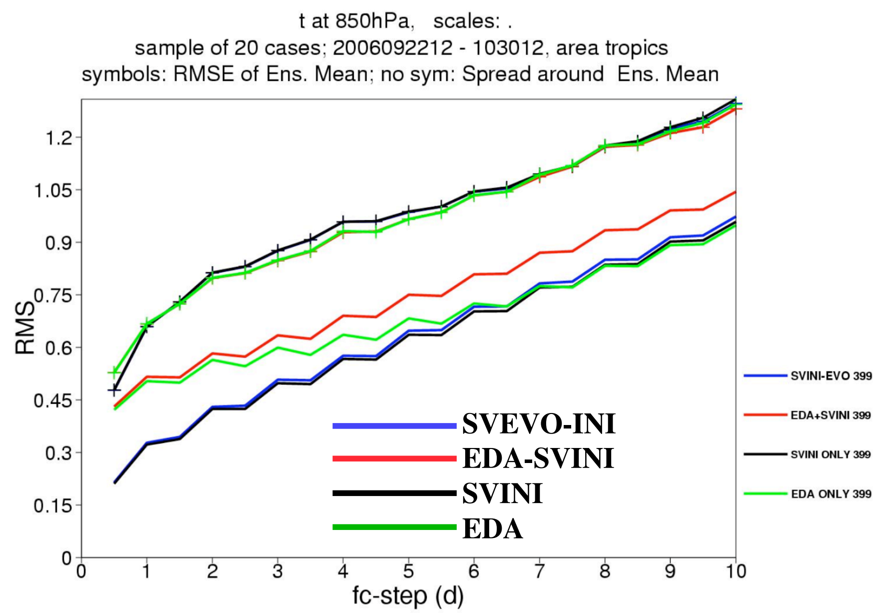

5. RPSS of EDA, SVINI, EDA-SVINI & SVEVO-INI EPS

The EDA-SVINI ensemble combines the benefits of the EDA and the SV techniques. Over the NH (left), the EDA-SVINI ensemble is only marginally better than the SVEVO-INI ensemble. But over the tropics (right), the EDA-SVINI ensemble has a higher RPSS. Note that the combination of EDA- and SVINI-based perturbations leads to an ensemble that outperforms one based on EDA-based perturbations only.

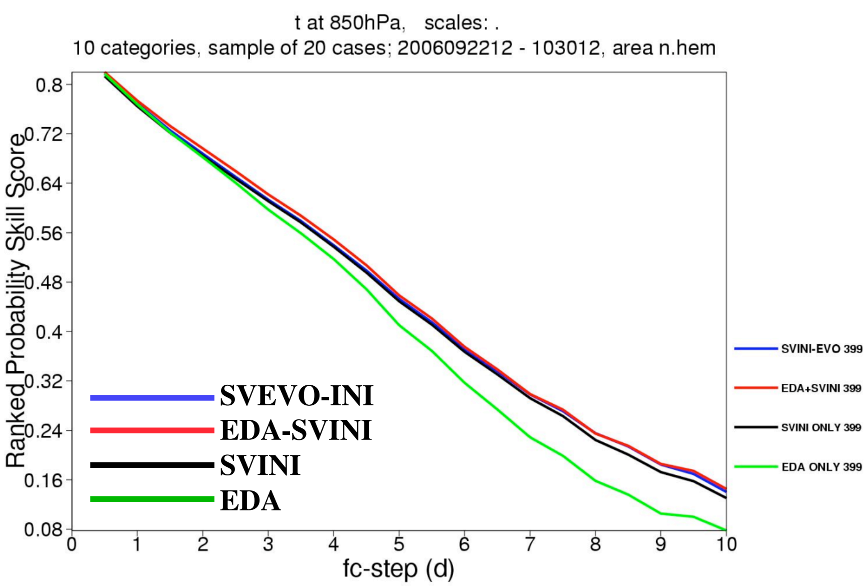

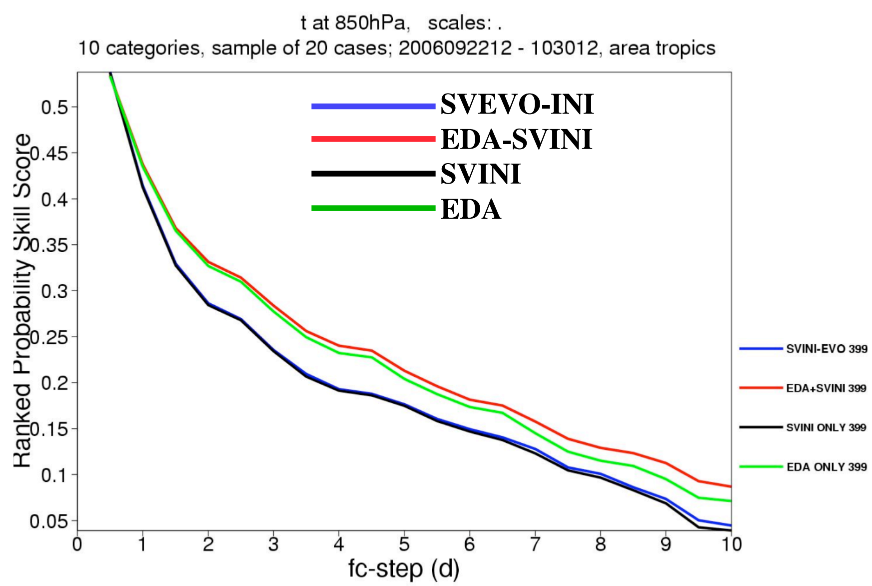

5. Conclusions

• The new 32-day VAREPS/monthly system (implemented on 11 March 2008) has been described. It includes 51 members, and run twice a-day (at 00 and 12 UTC) with a variable resolution, T_L399L62 up to day 10 and T_L255L62 afterwards (day 15 or 32). The 00 UTC ensemble runs with a coupled ocean from day 10 and once a-week (Thursday) is extended to 32-day. The new system provides users with seamless probabilistic forecasts from few weeks to few hours ahead.

• The average performance of the new system has been discussed, and its value in predicting severe weather events has been illustrated.

• Preliminary results on the potential use of an ensemble of analyses in the ensemble system has been discussed. Results have shown that combining SV- and EDA-based perturbations improve the performance of the ensemble system, especially in the tropics and for shorter forecast times.

Acknowledgements

The success of the ECMWF EPS is the result of the continuous work of ECMWF staff, consultants and visitors who had continuously improved the ECMWF model, analysis, diagnostic and technical systems, and of very successful collaborations with its member states and other international institutions. The work of all contributors is acknowledged.

Bibliography

On the ECMWF Ensemble Prediction System

- Buizza, R, & Palmer, T N, 1995: The singular vector structure of the atmospheric general circulation. *J. Atmos. Sci.*, 52, 1434-1456.
- Buizza, R, & Hollingsworth, A, 2002: Storm prediction over Europe using the ECMWF Ensemble Prediction System. *Meteorol. Appl*., 9, 1-17.
- Buizza, R., Leutbecher, M., & Isaksen, L., 2008: Potential use of an ensemble of analyses in the ECMWF ensemble prediction system. *Q. J. R. Meteorol. Soc.,* submitted.
- Buizza, R, Bidlot, J-R, Wedi, N, Fuentes, M, Hamrud, M, Holt, G, & Vitart, F, 2007: The new ECMWF VAREPS. *Q. J. Roy. Meteorol. Soc*., 133, 681-695.
- Coutinho, M M, Hoskins, B J, & Buizza, R, 2004: The influence of physical processes on extratropical singular vectors. *J. Atmos. Sci*., 61, 195-209.
- Hoskins, B J, Buizza, R, & Badger, J, 2000: The nature of singular vector growth and structure. *Q. J. R. Meteorol. Soc*., 126, 1565-1580.
- Molteni, F, Buizza, R, Palmer, T N, & Petroliagis, T, 1996: The new ECMWF ensemble prediction system: methodology and validation. *Q. J. R. Meteorol. Soc.*, 122, 73-119.
- Leutbecher, M & Palmer, T N, 2008: Ensemble forecasting. *J. Comp. Phys.*, 227, 3515-3539.
- Park, Y-Y, Buizza, R, & Leutbecher, M, 2008: TIGGE: preliminary results on comparing and combining ensembles. *Q. J. R. Meteorol. Soc*., in press.